Spring 2021

Neogene dinoflagellate cysts from the tropical americas

Damian Cardenas

Department: Geosciences and Geological and Petroleum Engineering

NEOGENE DINOFLAGELLATE CYSTS FROM THE TROPICAL AMERICAS

by

DAMIAN CARDENAS LOBOGUERRERO

A DISSERTATION

Presented to the Graduate Faculty of the

MISSOURI UNIVERSITY OF SCIENCE AND TECHNOLOGY

In Partial Fulfillment of the Requirements for the Degree

DOCTOR OF PHILOSOPHY

in

GEOLOGY AND GEOPHYSICS

2021

Approved by:

Francisca Oboh-Ikuenobe, Advisor
Lucy Edwards
John Hogan
Jonathan Obrist-Farner
Wan Yang

PUBLICATION DISSERTATION OPTION

This dissertation consists of the following two articles, formatted in the style used by the Missouri University of Science and Technology:

Paper I, found on pages 2–41, has been published in *Palaeogeography, Palaeoclimatology, Palaeoecology*.

Paper II, found on pages 42–64, has been submitted to *Review of Palaeobotany and Palynology*.

ABSTRACT

Marine palynomorphs, mainly dinoflagellate cysts and acritarchs, constitute excellent proxies for biostratigraphic and paleoceanographic studies in neritic sequences. Neogene marine palynological studies have mostly focused on the Northern Hemisphere, resulting in the scarcity of dinoflagellate cysts and acritarchs from tropical latitudes. Forty samples encompassing the late Chattian–late Burgidalian time interval (~24.1–17.3 Ma) in the Southern Caribbean were analyzed for their marine palynological contents. A biostratigraphic scheme for the region is proposed and includes the upper Chattian–lower Aquitanian *Minisphaeridium latirictum* Interval Zone (~23.9–22.0 Ma), the upper Aquitanian *Achomosphaera alcicornu* Interval Zone (~22.0–20.3 Ma), and the Burdigalian *Cribroperidinium tenuitabulatum* Interval Zone (~20.3–17.5 Ma). Two peridinioid dinoflagellate cyst species, *Cristadinium lucyae* sp. nov., and *Trinovantedinium uitpensis* sp. nov., and the acritarch *Quadrina*? *triangulata* sp. nov. are formally described. A conspicuous shift from a peridinioid-dominated dinoflagellate cyst assemblage to a gonyaulacoid-dominated assemblage occurs near the Aquitanian–Burdigalian boundary (~20.7 Ma), indicating a reduction in marine primary productivity. This paleoproductivity shift is linked to the initial constriction of the Central American Seaway—the oceanic pathway along the tectonic boundary between the South American plate and the Panama microplate.

ACKNOWLEDGMENTS

I would like to express my sincere gratitude and appreciation to my advisor, Dr. Francisca Oboh-Ikuenobe, for her invaluable support, mentorship and guidance during the last four years.

I am also deeply grateful to my dissertation committee members—Dr. Lucy Edwards, Dr. Wan Yang, Dr. John Hogan, and Dr. Jonathan Obrist-Farner—for providing constructive comments and suggestions throughout my Ph.D. studies.

I am especially indebted to Dr. Carlos Jaramillo for his insightful mentorship, which has had a remarkable impact on my formation as an early career scientist during the last six years.

I would like to thank all my friends and colleagues at Missouri S&T for their very generous assistance, especially Walaa Awad, Marissa Spencer, Erdoo Mongol, Olufeyisayo Ilesanmi, Onema Adojoh, and Aitalokhai Edegbai.

I acknowledge partial funding from the Missouri S&T Geology and Geophysics Program (Alfred Spreng Research Award), the Geological Society of America (GSA Graduate Student Research Grant), and the Paleontological Society (Yochelson Student Research Award).

Finally, I am most grateful to my family, especially my mom and grandma, for their unconditional support throughout all of my endeavors; I would not be where I am without their love, encouragement, and wisdom.

TABLE OF CONTENTS

LIST OF ILLUSTRATIONS

PAPER I Page

PAPER II

1. INTRODUCTION

Palynology is the branch of paleontology dealing with organic-walled microfossils, also known as palynomorphs. The terrestrial palynomorphs include mainly pollen and spores while the marine palynomorphs are mainly dinoflagellate cysts (dinocysts) and acritarchs. This dissertation documents a comprehensive marine palynological analysis of an early Miocene section located in the Colombian Caribbean Margin. Due to the scarcity of marine palynological studies in the tropical Americas, the aims of this research are to: (1) calibrate dinocyst and acritarch biostratigraphic events in the Colombian Caribbean Margin; (2) propose a provisional biostratigraphic scheme for the region; (3) reconstruct changes in paleoproductivity in the Southern Caribbean; and (4) formally described three new taxa.

Two peer-reviewed scientific articles resulted from this PhD research and are compiled in this dissertation. The paper entitled "Early Miocene marine palynology of the Colombian Caribbean Margin: biostratigraphic and paleoceanographic implications" was published in the journal *Palaeogeography, Palaeoclimatology, Palaeoecology*. The paper entitled "New peridinioid dinoflagellate cyst and acritarch taxa from the Miocene of Colombia, northwestern South America" has been submitted to the journal *Review of Palaeobotany and Palynology*.

PAPER

I. EARLY MIOCENE MARINE PALYNOLOGY OF THE COLOMBIAN CARIBBEAN MARGIN: BIOSTRATIGRAPHIC AND PALEOCEANOGRAPHIC IMPLICATIONS

Damián Cárdenas, Carlos Jaramillo, Francisca Oboh-Ikuenobe

Department of Geosciences and Geological and Petroleum Engineering, Missouri University of Science and Technology, Rolla, MO 65409

ABSTRACT

Dinoflagellate cysts and acritarchs are excellent proxies for biostratigraphic and paleoceanographic studies in neritic sequences. However, Neogene marine palynological studies in tropical latitudes are scarce. Here, we analyzed the marine palynological contents (dinoflagellate cysts, acritarchs, foraminiferal test linings and prasinophytes) of 40 samples from a well drilled in northernmost Colombia, southern Caribbean Sea, spanning the late Chattian–late Burgidalian time interval (~24.1–17.3 Ma). We propose a biostratigraphic scheme that includes an upper Chattian–lower Aquitanian *Minisphaeridium latirictum* Interval Zone (~23.9–22.0 Ma), an upper Aquitanian *Achomosphaera alcicornu* Interval Zone (~22.0–20.3 Ma), and a Burdigalian *Cribroperidinium tenuitabulatum* Interval Zone (~20.3–17.5 Ma). Our results reveal several biostratigraphic events that are heterochronous compared to high latitudes. Furthermore, the conspicuous shift from a peridinioid-dominated to a gonyaulacoid-dominated dinoflagellate cyst assemblage towards the Aquitanian–Burdigalian boundary

(~20.7 Ma) indicates a reduction in marine primary productivity. This paleoproductivity decline was probably driven by the initial constriction of the Central American Seaway.

1. INTRODUCTION

The Caribbean Sea is an oligotrophic, semi-enclosed (Atlantic net inflow ~28 × 106 m3 s−1), tropical sea characterized by small seasonal variability in sea surface temperature (~2.5 °C) and sea surface salinity (~0.5–1 psu) (Colón, 1963; Gordon, 1966; Müller-Karger et al., 1989; Johns et al., 2002). The emergence of the Panama Isthmus during the Neogene played a major role in the formation of the Caribbean Sea. The 12–10 Ma closure of the Central American Seaway—the oceanic pathway along the tectonic boundary between the South American plate and the Panama microplate—completely ceased the inflow of Pacific deep and intermediate waters into the proto-Caribbean (Jaramillo, 2018 and references therein). Foraminifera faunas reveal a subsequent disruption during the late Miocene (~10–7 Ma), lasting ~2.5 Ma, which appeared to have temporarily interrupted the circulation between Pacific and Caribbean shallow waters (Duque-Caro, 1990; Collins et al., 1996). The complete emergence of the Panama Isthmus during the Pliocene (~4.2–3.5 Ma) completely terminated the inflow of Pacific shallow waters into the Caribbean (Jaramillo, 2018 and references therein). Isotopic data indicate that modern oceanographic conditions in the Caribbean Sea are apparently driven by the full emergence of the Isthmus (Keigwin, 1982; Haug and Tiedemann, 1998; Haug et al., 2001; Gussone et al., 2004; Steph et al., 2006; Groeneveld et al., 2008). However, the role of (1) reduction in freshwater discharge into the Caribbean in response

to the Miocene reorganization of fluvial drainage basins in northern South America (e.g., proto-Amazon, proto-Orinoco), and (2) the onset of glaciations and its impact on precipitation across the Caribbean remain unknown (Jaramillo, 2018).

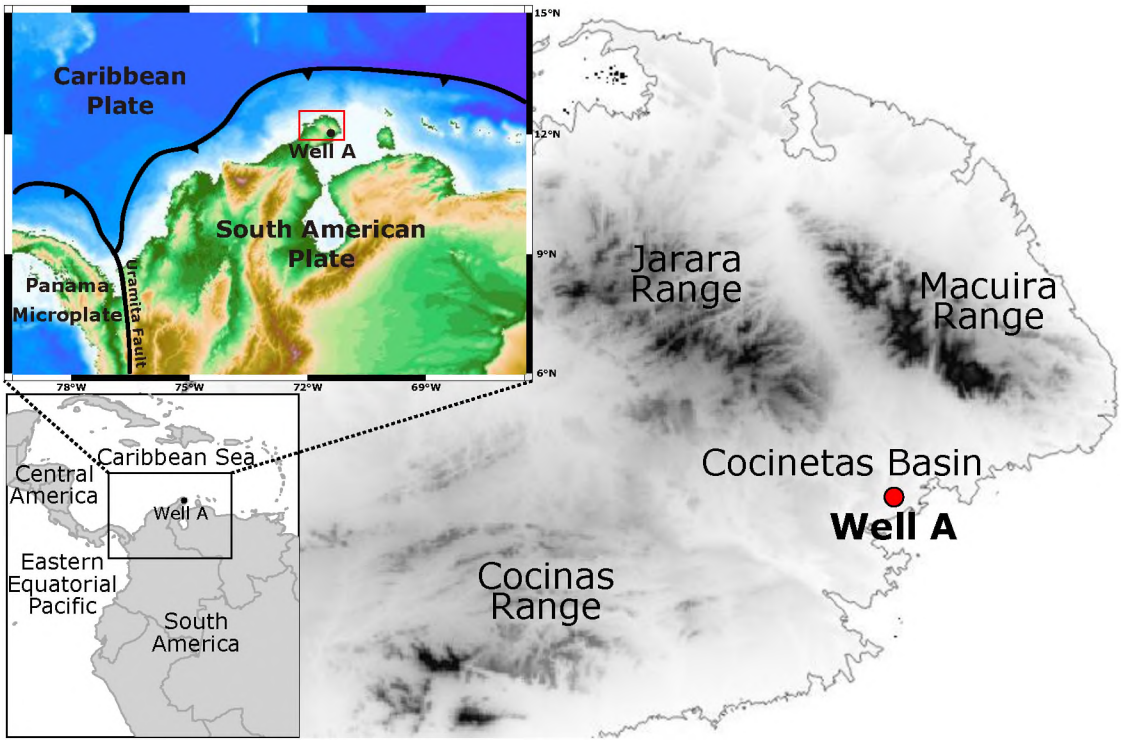

Figure 1. Location map of Well A in the Cocinetas Basin, northwestern South America, showing major tectonic boundaries and topographic features.

Neogene marine palynomorphs (mainly dinoflagellate cysts and acritarchs) have been widely used for biostratigraphic and paleoenvironmental studies in neritic sequences in temperate latitudes, especially in the Northern Hemisphere (e.g., De Schepper et al., 2017; Schreck et al., 2017). However, there is a large latitudinal sampling bias due to the limited number of Neogene marine palynological studies in tropical latitudes (Boyd et al., 2018). To date, only a few Neogene dinoflagellate cyst and acritarch taxa from

northwestern South America have been reported in the literature (e.g., Hoorn, 1993, Hoorn, 1994; Helenes and Cabrera, 2003; Boonstra et al., 2015; Jaramillo et al., 2017, 2020; Parra et al., 2019; da Silva-Caminha et al., 2020), since most Neogene palynological studies in the region have mainly focused on terrestrial palynomorphs. Among these palynological studies, Helenes and Cabrera (2003), Jaramillo et al. (2017) and Jaramillo et al. (2020) primarily analyzed marine palynomorph taxa for biostratigraphic purposes. Although two detailed Neogene marine palynological studies have been published for the Pacific region (Zegarra and Helenes, 2011; Duque-Herrera et al., 2018), none exists for the Caribbean region. Here, we present the first detailed late Chattian–late Burdigalian (~24.1–17.3 Ma) marine palynological study for the Colombian Caribbean Margin, and discuss its biostratigraphic and paleoceanographic implications for the Caribbean region.

2. GEOLOGICAL SETTING

The Colombian Caribbean Margin in northwestern South America is located along the tectonic boundary between the Caribbean and South American tectonic plates (Figure 1). Since the middle to late Eocene, several pull-apart sedimentary basins have developed along the northwestern margin of South America due to east-west displacement between these two tectonic plates (Macellari, 1995). One of these pull-apart basins, Cocinetas, is located in the Guajira Peninsula, the northernmost geographic feature of South America (Figure 1). The Cocinetas Basin in the southeastern Colombian Caribbean Margin is bounded by the Cocinas, Jarara, and Macuira ranges (Renz, 1960;

Figure 1). Cocinetas records a thick Eocene–Pliocene sedimentary sequence deposited in shallow to marginal marine to fluvial environments (Renz, 1960; Rollins, 1965; De Porta, 1974), and comprises the Eocene Macarao Formation; the Oligocene Siamana Formation; the lower to middle Miocene Uitpa, Jimol and Castilletes formations; and the upper Pliocene Ware Formation (Rollins, 1965; Moreno et al., 2015; Figure 2).

Well A (WA) is located in the Cocinetas Basin (11°56′38”N, 71°22′03”W) (Figure 1). The Oligocene–Miocene boundary is recognized in WA at 762 m (2500′) based on the last appearance datum (LAD) of the spore *Cicatricosisporites dorogensis*, dated as 23.03 Ma (Jaramillo et al., 2011, 2020). Placement of the Miocene-Oligocene boundary in WA is also supported by the LAD of the calcareous nannofossil *Helicosphaera recta* at 734.6 m (2410′), the LAD of the planktonic foraminifera *Ciperoella ciperoensis* at 752.9 m (2470′), and the LAD of the dinoflagellate cyst *Chiropteridium galea* at 856.5 m (2810′) (Jaramillo et al., 2020). In addition, strontium isotope chronostratigraphic data was extrapolated from the La Tienda section (Locality ID 290432), ~400 m northwest of WA (Hendy et al., 2015; Moreno et al., 2015; Jaramillo et al., 2020). The detailed calibration of WA can be found in Jaramillo et al. (2020). The 945–885 m (3100′–2905′) interval comprises the uppermost part of the Oligocene Siamana Formation, whereas the uppermost 885 m (2905′) interval corresponds to the lower Miocene Uitpa and Jimol formations (Figure 2). The Siamana Formation in WA (upper Chattian) consists of limestone interbedded with claystone and minor sandstone and siltstone (Figure 2). The late Chattian–late Aquitanian (~24.2–19.4 Ma) Uitpa Formation consists of a 492 m (1615′) thick sequence comprising mostly claystone and mudstone with interbedded sandstone and limestone towards the base (Figure 2). Lastly,

WA encompasses the lower and middle part of the Jimol Formation (late Aquitanian–late Burdigalian; ~19.4–17.3 Ma), which consists of a 354 m (1160′) thick sequence comprising interbedded sandstone and limestone with minor claystone interbeds towards the upper and lower parts of the sequence (Figure 2).

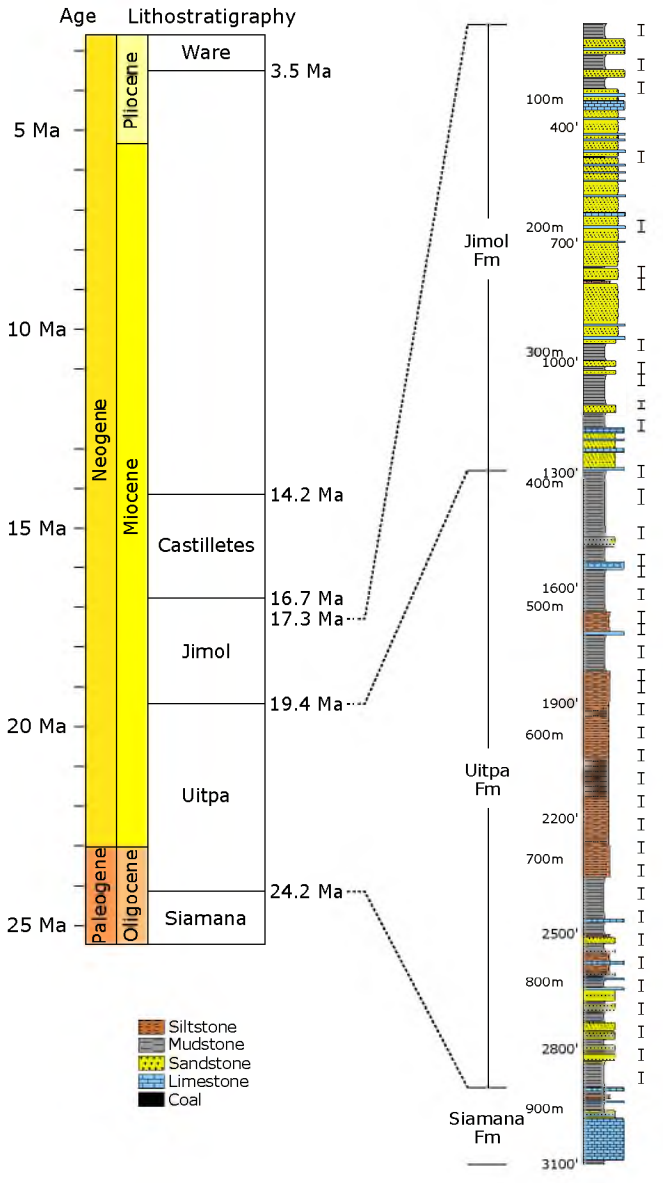

Figure 2. Chrono-lithostratigraphy for the Cocinetas Basin (after Moreno et al., 2015), lithostratigraphic column of Well A, and stratigraphic distribution of palynological samples.

Interpretations of depositional environments in the Cocinetas Basin indicate a shallowing-upward siliciclastic-dominated succession during the early Miocene, ranging from Uitpa middle and outer shelf deposits (100–200 m water-depth) (Hendy et al., 2015; Carrillo-Briceño et al., 2016) to Jimol shoreface and inner shelf deposits (<50 m water-depth) (Moreno et al., 2015) (Figure 2).

3. MATERIALS AND METHODS

Forty ditch-cutting samples spanning the 945–40 m (3100′–130′) interval in WA were sampled for palynology. Approximately 15 to 20 g per sample were processed following standard acid-based palynological techniques to remove carbonates and silicates using HCl and HF, respectively (Wood et al., 1996). Two coverslips smeared with unoxidized and oxidized residues were mounted per slide. Marine palynomorphs—acritarchs, dinoflagellate cysts (hereafter referred to as dinocysts), foraminiferal test linings and prasinophytes—and subordinate freshwater/brackish algae were identified and counted only in the unoxidized coverslip to avoid bias in the record of sensitive dinocysts to oxidation (e.g., peridinioid dinocysts). A Nikon E100 microscope was used for routine analysis of marine palynomorphs, while photomicrographs of selected taxa were taken using a Nikon Eclipse 50iPOL microscope coupled to a DS-Fi3 camera. Dinocyst taxonomy followed the Lentin and Williams Index of fossil dinoflagellates (Fensome et al., 2019). The stratigraphic column was done using the SDAR R package (Ortiz et al., 2019), whereas palynostratigraphic results were plotted using the analogue R

package (Simpson and Oksanen, 2020). Slides are housed at the Smithsonian Tropical Research Institute, Panama.

3.1. PALEOPRODUCTIVITY

The Peridinioid/Gonyaulacoid ratio, known as the P/G ratio, was calculated as the number of peridinioid dinocysts divided by the sum of gonyaulacoid and peridinioid dinocysts (e.g., Versteegh, 1994; Lammertsma et al., 2018). Samples with counts of <50 dinocysts were excluded from the analysis. This ratio, ranging between 0 and 1, was used to estimate fluctuations in paleoproductivity, as dinoflagellates are sensitive to changes in nutrient availability. Based on observations of the life-styles and feeding strategies of modern thecate dinoflagellates, two extant genera are considered analogs for gonyaulacoid and peridinioid cysts: the autotrophic genus *Gonyaulax* represents the extant order Gonyaulacales, whereas the heterotrophic genus *Protoperidinium* represents the extant order Peridiniales (Powell et al., 1992). Gonyaulacoid and peridinioid cysts are thus considered to represent mostly autotrophic and heterotrophic dinoflagellates, respectively. Consequently, P/G values that tend towards 0 indicate low nutrient availability while P/G values that tend towards 1 indicate high nutrient availability.

3.2. TERRESTRIAL INPUT

The Terrestrial/Marine (T/M) index was calculated as the number of terrestrial palynomorphs divided by the sum of terrestrial and marine palynomorphs. The proportion of pollen and spores relative to the total palynological assemblage is a proxy for estimating terrestrial influence in marine environments (e.g., Versteegh, 1994; Zwiep et

al., 2018). Marine palynomorphs include acritarchs, dinocysts, foraminiferal test linings and prasinophytes. Pollen and spore data in WA are derived from Jaramillo et al. (2020). Samples with less than 150 total palynomorphs were excluded from the analysis.

3.3. STATISTICAL ANALYSIS

Comparisons between the means of two unpaired groups were achieved using the two-sided Welch t-test to account for unequal variances between the compared groups (Dalgaard, 2008); P values (p) and degrees of freedom (df) are provided. Nonparametric correlation tests between two variables were achieved using the Spearman rank to account for monotonic (increasing or decreasing) relationship between the compared variables (Dalgaard, 2008); Spearman coefficients (ρ) and P values (p) are provided. Non-metric multidimensional scaling (nMDS) was performed to compare species composition between palynological assemblages among samples using the Bray-Curtis dissimilarity; the fit of the regression between ordination-based distances and predicted values (stress) is provided (Kruskal, 1964). The analysis of similarities (ANOSIM) was conducted to test the statistical significance between compared palynological assemblages (Clarke, 1993); the ANOSIM statistic (R) and significance (P) values are provided. All statistical analyses were performed using R (R Core Team, 2017). The nMDS and ANOSIM analyses were performed using the Vegan R package (Oksanen et al., 2019).

4. RESULTS

Palynological samples yielded a moderate to good recovery of well-preserved marine palynomorphs (mean count per sample: 218.7, sd: 93.9, n: 34), except in the 399–241 m (1310′–790′) interval (mean: 45.8, sd: 11.5, n: 6). The marine palynological assemblage consists of taxa identified as 24 peridinioid dinocysts, 23 gonyaulacoid dinocysts, 11 acritarchs, 2 prasinophytes, and 15 reworked dinocysts (Appendix 1).

4.1. BIOSTRATIGRAPHY

Several dinocyst and acritarch biostratigraphic events were identified in WA, and calibrated with biostratigraphy (calcareous nannofossils, palynomorphs and planktonic foraminifera) and Sr chronostratigraphy in the Cocinetas Basin (Hendy et al., 2015; Jaramillo et al., 2020). These biostratigraphic events include mostly last appearance datums (LADs). We avoided using first appearance datums (FADs) as much as possible because they may be biased by caving since ditch-cutting samples were studied.

Cristadinium sp. of De Verteuil and Norris, 1992, *Echinidinium euaxum*, *Incertae sedis* B, *Lejeunecysta marieae*, *Quadrina*? *condita*, *Sumatradinium hispidum*, *Sumatradinium soucouyantiae*, *Trinovantedinium papula*, and *Trinovantedinium*? *xylochoporum* occur consistently in the upper Chattian and Aquitanian, whereas *Cleistosphaeridium diversispinosum*, *Incertae sedis* C and *Selenopemphix nephroides* occur consistently throughout the entire sequence (upper Chattian–upper Burdigalian) (Figure 3, Appendix 1). The LAD of *Minisphaeridium latirictum* occurs in the Aquitanian at ~21.9 Ma (652.3 m; 2140′). The LAD of *Achomosphaera alcicornu* at

~20.3 Ma (487.7 m; 1600′) occurs near the Aquitanian–Burdigalian boundary (Figure 3, Figure 4). The LADs of *Cristadinium* sp. of De Verteuil and Norris, 1992, *Quadrina* "incerta" of Jaramillo et al., 2017, and *Cribroperidinium tenuitabulatum* occur in the Burdigalian at ~18.9 Ma (307.8 m; 1010′), ~17.6 Ma (85.3 m; 280′), and ~ 17.5 Ma (67.1 m; 220′), respectively (Figure 3, Figure 4).

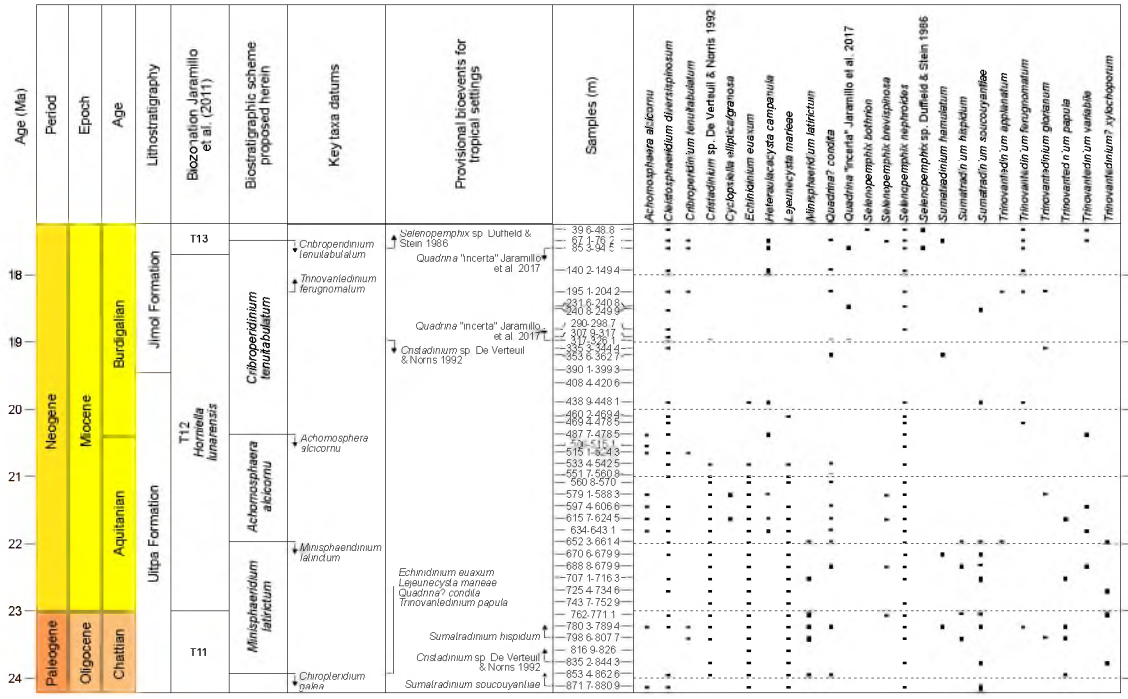

Figure 3. Proposed biostratigraphic scheme for the Colombian Caribbean Margin in relation to the palynological zonation for the Colombian Llanos Basin (Jaramillo et al., 2011), showing biostratigraphic events (last appearance datum [LAD]; first appearance datum [FAD]) and ranges of selected marine palynomorphs in Well A.

The stratigraphic occurrences of *Quadrina* "incerta" of Jaramillo et al., 2017, *Selenopemphix* sp. D of Duffield and Stein, 1986 and *Trinovantedinium ferugnomatum* are restricted to the Burdigalian (Figure 3, Appendix 1). Reworked dinocysts are restricted to the upper Chattian–lower Burdigalian (Figure 5, Appendix 1).

Although first appearances in WA may be biased due to caving, we assume minimal caving in the uppermost part of the drilled sequence. Therefore, we consider that the FADs of (1) *Quadrina* "incerta" of Jaramillo et al., 2017 at ~19.0 Ma (326.1 m; 1070′), (2) *Trinovantedinium ferugnomatum* at ~18.3 Ma (204.2 m; 670′), and (3) *Selenopemphix* sp. D of Duffield and Stein, 1986 at ~17.6 Ma (94.5 m; 310′) to be reliable (Figure 3, Figure 4).

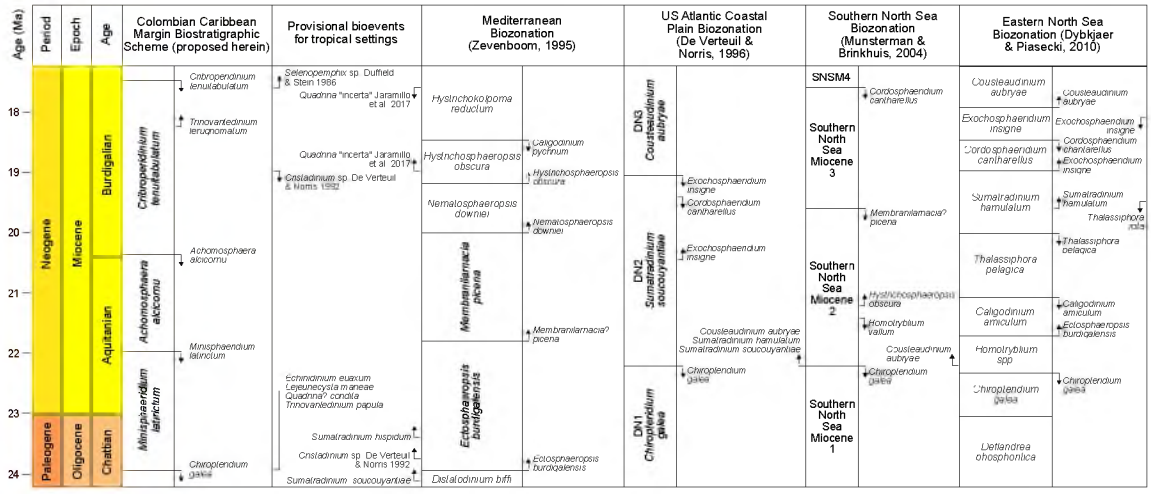

Figure 4. Schematic comparison of lower Miocene biostratigraphic zones and marine palynological events between the Colombian Caribbean Margin and the Northern Hemisphere.

We correlate WA biostratigraphy with the Cenozoic palynological zonation for the Colombian Llanos Basin (Jaramillo et al., 2011) (Figure 3). We also compare the proposed biostratigraphic scheme to calibrated marine palynological zonations and biostratigraphic events for the Northern Hemisphere, including the western North Atlantic (De Verteuil and Norris, 1996), the Mediterranean (Dybkjær and Piasecki,

2010), and the North Sea (Munsterman and Brinkhuis, 2004; Zevenboom, 1995) (Figure 4).

4.2. PALEOPRODUCTIVITY

The nMDS analysis shows a significant difference in dinocyst community composition (ANOSIM: $R = 0.60$, $P = 0.001$) between the 881–533 m (2890′–1750′) and the 524–40 m (1720′–130′) intervals (Figure 6). The lower interval (881–533 m; 2890′–1750′), late Chattian and most of the Aquitanian (~24.1–20.8 Ma), is dominated by heterotrophic peridinioid dinocyst taxa, including *Brigantedinium*, *Cristadininium*, *Echinidinium*, *Lejeunecysta*, *Selenopemphix*, *Sumatradinium* and *Trinovantedinium* species (Figure 5). The upper interval (524–40 m; 1720′–130′), uppermost Aquitanian and Burdigalian (~20.6–17.3 Ma), is dominated by autotrophic gonyaulacoid dinocyst taxa, mostly *Hystrichokolpoma rigaudiae*, *Lingulodinium machaerophorum*, *Operculodinium centrocarpum* and *Spiniferites ramosus* (Figure 5). The P/G ratio is significantly higher (t-test: $p < 0.01$, df: 24.98) during the lower interval (median: 0.59, sd: 0.26, n: 20) compared to the upper interval (median: 0.11, sd: 0.09, n: 14) (Figure 5). In addition, foraminiferal test linings are more abundant (t-test: $p < 0.01$, df: 22.22) in the lower interval (median: 41, sd: 20.83, n: 20) compared to the upper interval (median: 3.5, sd: 5.15, n: 14) (Figure 5). The Terrestrial/Marine (T/M) index shows no significant difference (t-test: $p = 0.11$, df: 10.12) between the lower interval (median: 0.37, sd: 0.10, n: 9) and the upper interval (median: 0.49, sd: 0.20, n: 8). There is also no significant correlation between the T/M index and the P/G ratio (Spearman $\rho = -0.31$, $p = 0.23$).

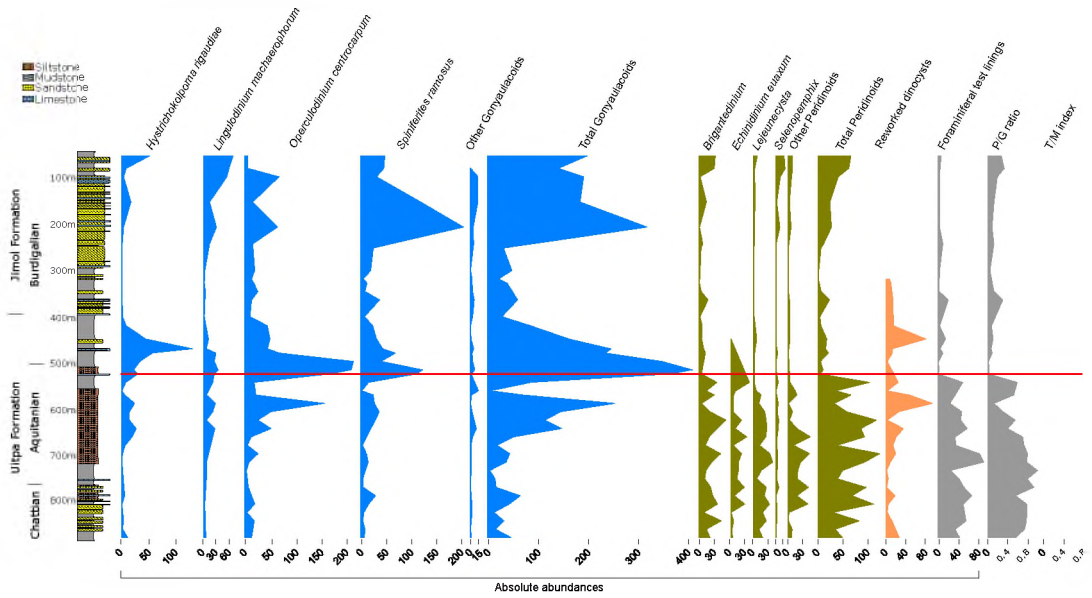

Figure 5. Absolute abundances of dinocysts and foraminiferal test linings in relation to the Peridinioid/Gonyaulacoid (P/G) ratio and the Terrestrial/Marine (T/M) index. Gonyaulacoid (mostly autotrophic) and peridinioid (mostly heterotrophic) taxa are shown in blue and green, respectively. Foraminiferal test linings and P/G ratio, semiquantitative proxies to reconstruct fluctuations in paleoproductivity, are shown in gray. Reworked dinocysts and T/M index are shown in orange and brown, respectively. The red line denotes both the turnover from peridinioid- to gonyaulacoid-dominated dinocyst assemblages and the sudden decrease in the abundance of foraminiferal test lining towards the Aquitanian–Burdigalian boundary. The gray box indicates a low recovery interval (<50 dinocysts).

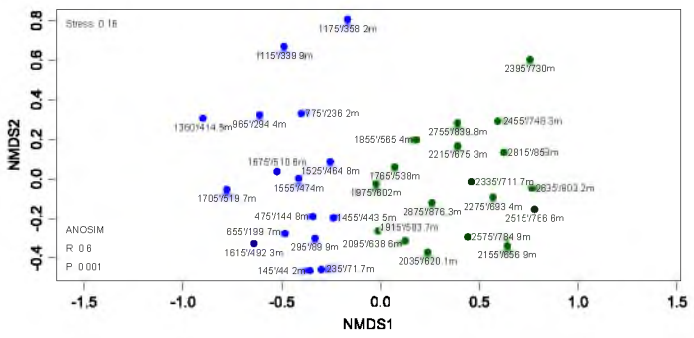

Figure 6. Non-metric multidimensional scaling (nMDS) ordination plot for the dinocyst assemblages in Well A, based on Bray-Curtis distance matrix. Each dot on the nMDS plot represents a palynological sample (average depth in feet/m indicated for each sample interval). Blue dots represent gonyaulacoid-dominated dinocyst assemblages in the upper Chattian and Aquitanian, whereas green dots represent peridinioid-dominated dinocyst assemblages in the Burdigalian.

5. DISCUSSION

5.1. A BIOSTRATIGRAPHIC SCHEME FOR THE COLOMBIAN CARIBBEAN MARGIN

The assumption that the timing of temperate dinocyst biostratigraphic events (e.g., FADs, LADs) could be considered as coetaneous at tropical latitudes needs to consider paleobiogeography. Biostratigraphic ranges of marine palynomorphs are often asynchronous worldwide due to differences in paleoceanographic conditions across latitudes (Williams et al., 2004). Previous palynological studies in the Caribbean region have demonstrated the asynchrony of events compared to those in Oligocene–Miocene zonations for mid- and high latitudes (Helenes and Cabrera, 2003; Jaramillo et al., 2020). Here, we propose a biostratigraphic scheme for the lower Miocene in the Colombian Caribbean Margin (Figure 3), which could serve as a baseline to establish a Neogene marine palynological zonation for the tropical Americas.

The upper Chattian–upper Burdigalian interval in the Cocinetas Basin is divided, from base to top, into three dinocyst zones that are discussed below (Figure 3).

Minisphaeridium latirictum Interval Zone. Definition: The *M. latirictum* biozone is defined by the LAD of *Chiropteridium galea* at the base and the LAD of *Minisphaeridium latirictum* at the top.Age: Late Chattian to early Aquitanian (23.9 to 22.0 Ma).Characteristic taxa: This biozone is characterized by the occurrence of *Cleistosphaeridium diversispinosum*, *Cristadinium* sp. of De Verteuil and Norris, 1992, *Echinidinium euaxum*, *Echinidinium* sp., *Incertae sedis* B, *Lejeunecysta marieae*, *Minisphaeridium latirictum*, *Selenopemphix nephroides*, *Sumatradinium hispidum*, *Sumatradinium soucouyantiae*, *Trinovantedinium papula*, and *Trinovantedinium*?

xylochoporum.Comments: The LAD of *C. galea* in equatorial (23.98 Ma) and temperate (22.36 Ma) regions has been used as a key biostratigraphic marker for the placement of the Oligocene–Miocene boundary (Williams et al., 2004) and the definition of Neogene biozones (e.g., De Verteuil and Norris, 1996; Dybkjær and Piasecki, 2010). In WA, this event at 23.9 Ma is consistent with previous studies (Jaramillo et al., 2020). In contrast, although the LAD of *M. latirictum* in the Northern Hemisphere is constrained to the Tortonian (De Verteuil and Norris, 1996; Dybkjær and Piasecki, 2010; Fensome et al., 2009, Fensome et al., 2016; Schreck et al., 2012; Grøsfjeld et al., 2019), its stratigraphic range in equatorial latitudes remains unknown. The continuous occurrence of *M. latirictum* in the lowermost part of WA suggests a mid-Aquitanian LAD (22.0 Ma) for this species in the Caribbean Colombian Margin.Correlation: The *M. latirictum* biozone (DN1) correlates with the uppermost part of the *Cicatricosisporites dorogensis* (T11) zone and the lowermost part of *Horniella lunarensis* (T12) zone in the Llanos Basin, Colombia (Jaramillo et al., 2011).Achomosphaera alcicornu Interval Zone. Definition: The *A. alcicornu* biozone is defined by the LAD of *Minisphaeridium latirictum* at the base and the LAD of *Achomosphaera alcicornu* at the top.Age: Middle to late Aquitanian (22.0 to 20.3 Ma).Characteristic taxa: This biozone is characterized by the occurrence of *Achomosphaera alcicornu*, *Cleistosphaeridium diversispinosum*, *Cristadinium* sp. of De Verteuil and Norris, 1992, *Cyclopsiella elliptica/granosa*, *Echinidinium euaxum*, *Heteraulacacysta campanula*, *Lejeunecysta marieae*, *Quadrina*? *condita*, *Selenopemphix brevispinosa*, *Selenopemphix nephroides*, *Trinovantedinium* sp., and *Trinovantedinium variabile*.Comments: The LAD of *A. alcicornu* is asynchronous between equatorial (27.0 Ma) and temperate (13.0 Ma) regions (Williams et al., 2004). Recent palynological

studies, however, indicate a younger LAD for this species in the tropical Americas (Pérez-Consuegra et al., 2018; Jaramillo et al., 2020). The continuous occurrence of *A. alcicornu* in the lower and middle part of WA suggests an early Burdigalian LAD (20.3 Ma) for this species in the Caribbean Colombian Margin.Correlation: The *A. alcicornu* biozone (DN2) correlates with the lower to middle *Horniella lunarensis* (T12) palynological zone in the Llanos Basin, Colombia (Jaramillo et al., 2011).Cribroperidinium tenuitabulatum Interval Zone. Definition: The C. *tenuitabulatum* biozone is defined by the LAD of *Achomosphaera alcicornu* at the base and the LAD of *Cribroperidinium tenuitabulatum* at the top.Age: Burdigalian (20.3 to 17.5 Ma).Characteristic taxa: This biozone comprises the FAD of *Trinovantedinium ferugnomatum* and is characterized by the occurrence of *Cleistosphaeridium diversispinosum*, *Cribroperidinium tenuitabulatum*, *Heteraulacacysta campanula*, *Paralecaniella indentata*, *Quadrina*? *condita*, *Quadrina* "incerta" of Jaramillo et al., 2017, *Selenopemphix nephroides*, *Sumatradinium hamulatum*, *Trinovantedinium applanatum*, *Trinovantedinium ferugnomatum*, and *Trinovantedinium glorianum*.Comments: The LAD of *C. tenuitabulatum* in the Colombian Llanos Basin, which is constrained to the mid-Burdigalian (17.48 Ma) based on foraminifera, carbon isotopes and magnetostratigraphy (Jaramillo et al., 2011), is consistent with the LAD for this species in WA at 17.5 Ma. In contrast, the stratigraphic range of *T. ferugnomatum* in the tropical Americas remains unclear, although this species was recently reported in Tortonian and Messinian deposits in the Colombian Pacific Margin (Duque-Herrera et al., 2018). The FAD of *T. ferugnomatum* in the Northern Hemisphere is constrained to the upper Burdigalian (Louwye et al., 2008); however, the continuous occurrence of this

species in the uppermost part of WA suggest a mid-Burdigalian FAD (18.3 Ma) in the Colombian Caribbean Margin, as the three sporadic occurrences of *T. ferugnomatum* at 19.9 Ma, 20.2 Ma, and 23.2 Ma most likely represent caving.Correlation: The *C. tenuitabulatum* biozone (DN3) correlates with the middle to upper *Horniella lunarensis* (T12) zone and the lowermost part of *Echitricolporites maristellae* (T13) zone in the Llanos Basin, Colombia (Jaramillo et al., 2011).

5.2. POTENTIAL KEY BIOSTRATIGRAPHIC MARKERS AND EVENTS IN TROPICAL SETTINGS

Several biostratigraphic studies using marine palynology have been carried out on Neogene sedimentary sequences in mid- and high latitudes, especially in the Northern Hemisphere; however, such studies in equatorial regions are scarce (Boyd et al., 2018). Calibration of Neogene dinocyst and acritarch events in the tropical Americas, therefore, is critical to elucidate the stratigraphic ranges of key taxa in equatorial regions. In addition to the biostratigraphic events discussed above (Section 5.1), the presence of several key taxa in WA implies that future marine palynological analysis of Oligocene and Miocene sections in the tropical Americas are needed to constrain the stratigraphic ranges, particularly FADs, of the following species, presented in alphabetical order:

Cristadinium sp. of De Verteuil and Norris, 1992: This informal protoperidinioid dinocyst (Figure 7D, E) has only been reported in Serravallian deposits in the western North Atlantic (De Verteuil and Norris, 1992, Plate 2, Figures 9–12; Edwards et al., 2018, Figure 5.4). The LAD of *Cristadinium* sp. of De Verteuil and Norris, 1992 in WA at 19.0 Ma and its continuous occurrence in the lower to middle part of WA suggests that

the stratigraphic range for this species spans at least from the Aquitanian to the lower Burdigalian in the Colombian Caribbean Margin (Figure 3, Figure 4).

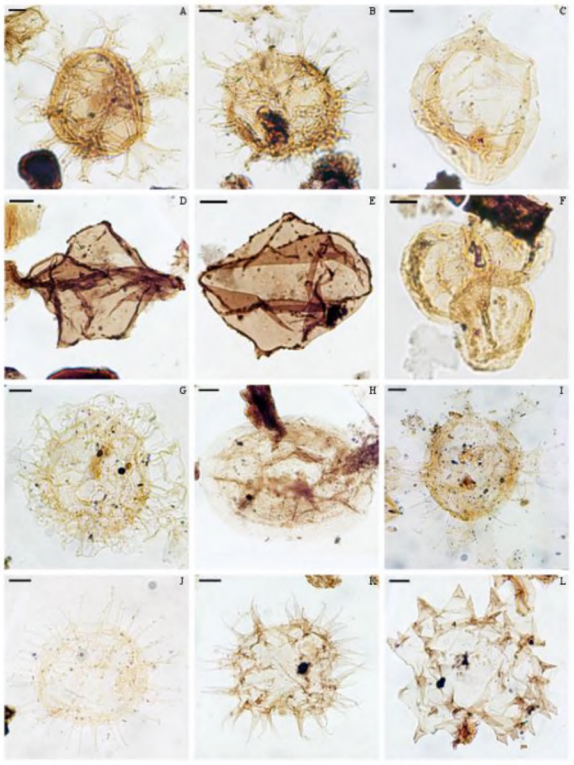

Figure 7. Photomicrographs of selected marine palynomorphs. Scale bar is 10 μm. EF: England Finder coordinates. (A) *Achomosphaera alcicornu*, uncertain view, low focus on processes. 1660′–1690′, EF: B37/3. (B) *Cleistosphaeridium diversispinosum*, apical view, low focus on processes. 1750′–1780′, EF: O39/2. (C) *Cribroperidinium tenuitabulatum*, dorsal view, high focus on archaeopyle margin and wall. 1690′–1720′, EF: F43/3. (D) *Cristadinium* sp. of De Verteuil and Norris, 1992, dorsal view, high focus on archaeopyle margin, cingulum and wall. 1750′–1780′, EF: V43/3. (E) *Cristadinium* sp. of De Verteuil and Norris, 1992, dorsal view, high focus on archaeopyle suture, cingulum and wall. 1810′–1840′, EF: T33. (F) *Cyclopsiella elliptica/granosa* complex, uncertain view, high focus on wall. 1900′–1930′, EF: H37/3. (G) Emmetrocysta? sp., apical view, low focus on processes and archaeopyle margin. 1510′–1540′, EF: N44/2. (H) *Heteraulacacysta campanula*, apical view, 2080′–2110′, low focus on archaeopyle margin and wall. EF: R30/4. (I) *Hystrichokolpoma rigaudiae*, apical view, low focus on processes and archaeopyle margin. 1690′–1720′, EF: V45. (J) *Polysphaeridium zoharyi*, uncertain view, high focus on processes and archaeopyle margin. 130′–160′, EF: X37/2. (K) *Quadrina*? *condita*, uncertain view, mid-focus on wall and processes. 1960′–1990′, EF: B28/4. (L) *Quadrina* "incerta" of Jaramillo et al., 2017, uncertain view, mid-focus on wall and processes. 280′–310′, EF: R37/2.

Echinidinium euaxum: This protoperidinioid dinocyst species of unknown affinity (Figure 9B) was originally reported in the Gulf of Mexico as *Multispinula* sp. in upper Burdigalian deposits (LeNoir and Hart, 1986, Plate 4, Figure 1) and *Multispinula* cf. *minuta* in Burdigalian–Messinian deposits (Duffield and Stein, 1986, Plate 1, Figure 7). The continuous occurrence of *E. euaxum* in the lower to middle part of WA suggests that the FAD of this species in the Colombian Caribbean Margin may extend at least to the Aquitanian (Figure 3, Figure 4).

Lejeunecysta marieae: The FAD of this protoperidinioid dinocyst species (Figure 9J) is constrained to the upper Burdigalian in the Northern Hemisphere (Louwye et al., 2008). However, the continuous occurrence of *L. marieae* in the lower to middle part of WA suggests that the FAD of this species in the Colombian Caribbean Margin may extend at least to the Aquitanian (Figure 3, Figure 4).

Quadrina? *condita*: This fossil acritarch species (Figure 7K), questionably assigned to the genus *Quadrina* Bujak in Bujak et al., 1980, was originally reported as *Incertae sedis* A in upper Burdigalian–Messinian deposits in the Gulf of Mexico (Duffield and Stein, 1986, Plate 2, Figure 4). Subsequently, De Verteuil and Norris (1992) described *Q. condita* and suggested that this species may correspond to a dinocyst, most likely protoperidiniacean (Soliman et al., 2012). Although recent palynological analyses in northwestern South America indicate a mid-Burdigalian FAD (Jaramillo et al., 2017), the continuous occurrence of *Q. condita* in WA suggests that the FAD of this species in the tropical Americas may extend at least to the Aquitanian (Figure 3, Figure 4).

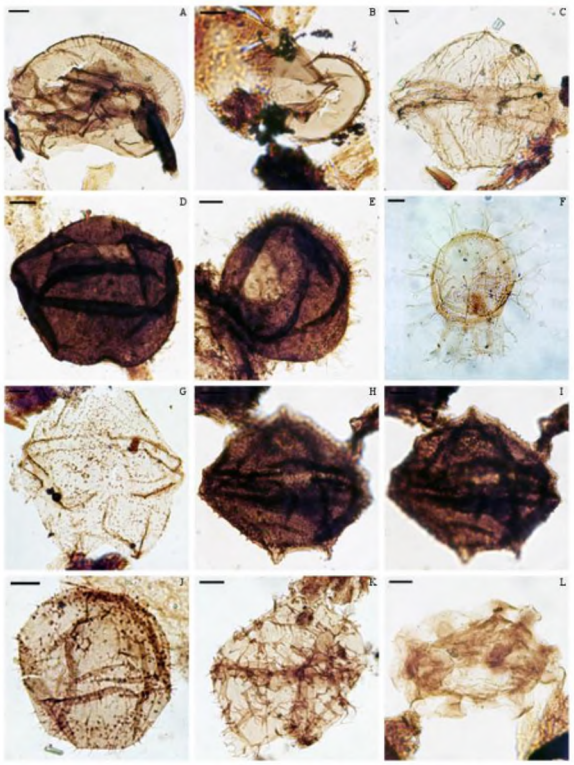

Figure 8. Photomicrographs of selected marine palynomorphs. Scale bar is 10 μm. EF: England Finder coordinates. (A) *Selenopemphix bothrion*, apical view, low focus on wall and archaeopyle margin. 2080′–2110′, EF: N32/4. (B) *Selenopemphix* sp. D of Duffield and Stein, 1986, apical view, mid-focus on cingular processes. 280′–310′, EF: J39/3. (C) *Sumatradinium hamulatum*, dorsal view, mid-focus on wall, processes and archaeopyle suture. 220′–250′, EF: J35/1. (D) *Sumatradinium hispidum*, dorsal view, mid-focus on wall, processes and archaeopyle margin. 2500′–2530′, EF: U30. (E) *Sumatradinium soucouyantiae*, dorsal view, mid-focus on wall, processes and archaeopyle margin. 2140′–2170′, EF: S35/3. (F) *Spiniferites mirabilis*, dorsal view, dorsoventral view, mid-focus on processes. 1160′–1190′, EF: P26. (G) *Trinovantedinium applanatum*, ventral view, low focus on processes, cingulum and archaeopyle margin. 640′–670′, EF: H30/1. (H) *Trinovantedinium glorianum*, ventral view, low focus on wall, processes and cingulum. 1900′–1930′, EF: O47/1. (I) *Trinovantedinium glorianum*, dorsal view, high focus on wall, processes and archaeopyle margin. 1900′–1930′, EF: O47/1. (J) *Trinovantedinium papula*, dorsal view, dorsoventral view, mid-focus on wall and processes. 2020′–2050′, EF: E31/4 (K) *Trinovantedinium*? *xylochoporum*, ventral view, mid-focus on wall and processes. 2140′–2170′, EF: V39/3. (L) *Tuberculodinium vancampoae*, apical view, low focus on archaeopyle margin and processes. 1960′–1990′, EF: P28/1.

Quadrina "incerta" of Jaramillo et al., 2017: This informal acritarch (Figure 7L) was originally reported as Dinocyst XI in upper Burdigalian deposits in the Gulf of Mexico (LeNoir and Hart, 1986, Plate 7, Figure 6) and subsequently recovered in mid-Burdigalian deposits in northwestern South America (Jaramillo et al., 2017, Figure S5D). Its continuous occurrence in the uppermost part of WA supports a middle to upper Burdigalian stratigraphic range in the tropical Americas (Figure 3, Figure 4). However, the FAD and LAD of this species require future calibration.

Selenopemphix sp. D of Duffield and Stein, 1986: This informal protoperidinioid dinocyst (Figure 8B) was originally reported in upper Aquitanian deposits in the Gulf of Mexico (Duffield and Stein, 1986, Plate 1, Figure 9). In contrast, its sporadic occurrence in the uppermost part of WA suggests an upper Burdigalian stratigraphic range in the Colombian Caribbean Margin (Figure 3, Figure 4). However, the FAD and LAD of this species require future calibration.

Sumatradinium hispidum: The FAD of this fossil protoperidinioid dinocyst species (Figure 8D) is constrained to the late Burdigalian in the Northern Hemisphere (De Verteuil, 1996; Louwye et al., 2008). In contrast, the continuous occurrence of *S. hispidum* in the lower part of WA suggests that the FAD of this species in the Colombian Caribbean Margin may extend at least to the Aquitanian (Figure 3, Figure 4).

Sumatradinium soucouyantiae: The FAD of this fossil protoperidinioid dinocyst species (Figure 8E) is constrained to the mid-Aquitanian in the Northern Hemisphere (Williams et al., 2004) and west-central Africa (Willumsen et al., 2014). However, its continuous occurrence in the lower part of WA suggest that its FAD in the Colombian Caribbean Margin may extend at least to the early Aquitanian (Figure 3, Figure 4).

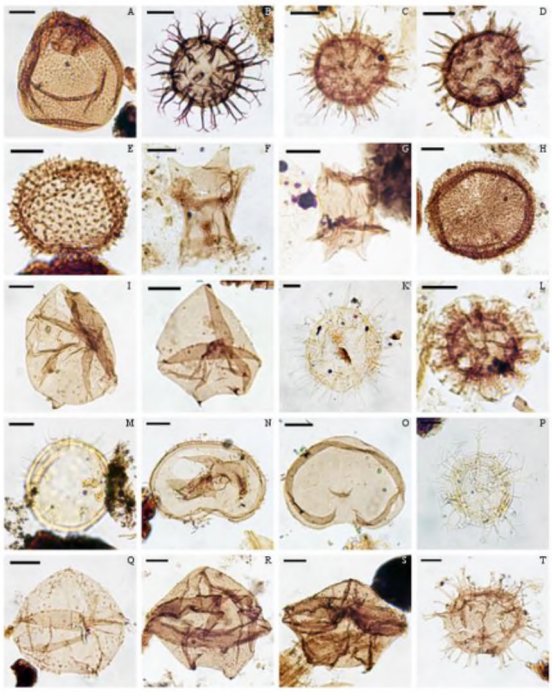

Figure 9. Photomicrographs of selected marine palynomorphs. Scale bar is 10 µm. EF: England Finder coordinates. (A) *Brigantedinium* sp., dorsal view, high focus on archaeopyle suture and wall. 130′–160′, EF: L44/3. (B) *Echinidinium euaxum*, apical view, low focus on processes and archaeopyle margin. 2080′–2110′, EF: H31/3. (C) *Echinidinium* sp., apical view, low focus on processes and archaeopyle margin. 2260′–2290′, EF: G35/4. (D) *Echinidinium* sp., apical view, high focus on processes and archaeopyle margin. 2500′–2530′, EF: W40/4. (E) *Incertae sedis* A, uncertain view, mid-focus on wall and processes. 1900′–1930′, EF: U28/2. (F) *Incertae sedis* B, ventral? view, low focus on wall and archaeopyle? suture. 2620′–2650′, EF: G30/2. (G) *Incertae sedis* B, dorsalventral? view, mid-focus on wall. 2260′–2290′, EF: S38/2. (H) *Incertae sedis* C, uncertain view, mid-focus on wall and processes. 2140′–2170′, EF: D43/2. (I) *Komewuia*? sp., dorsal view, low focus on archaeopyle margin and wall. 2020′–2050′, EF: U31/4. (J) *Lejeunecysta marieae*, dorsal view, mid-focus on archaeopyle suture and wall. 2080′–2110′, EF: X33/2. (K) *Lingulodinium machaerophorum*, apical view, high focus on processes and archaeopyle margin. 640′–670′, EF: B39/4. (L) *Minisphaeridium latirictum*, apical view, low focus on processes and archaeopyle margin. 2620′–2650′, EF: L41. (M) *Operculodinium centrocarpum*, dorsal view, low focus on archaeopyle margin, wall and processes. 280′–310′, EF: N40. (N) *Selenopemphix brevispinosa*, apical view, mid-focus on archaeopyle margin and cingular processes. 220′–250′, EF: R45/3. (O) *Selenopemphix nephroides*, apical view, mid-focus on archaeopyle suture and wall. 220′–250′, EF: L26/1. (P) *Spiniferites ramosus*, dorsal view, low focus on processes and archaeopyle margin. 130′–160′, EF: W47/2. (Q) *Trinovantedinium ferugnomatum*, dorsal view, 220′–250′, EF: J45. (R) *Trinovantedinium* sp., dorsal view, high focus on archaeopyle margin and wall. 2500′–2530′, EF: D38/1. (S) *Trinovantedinium* sp., ventral view, low focus on wall and cingulum. 2080′–2110′, EF: E42/3. (T) *Trinovantedinium variabile*, uncertain view, mid-focus on processes and wall. 220′–250′, EF: P32.

Trinovantedinium papula: This fossil protoperidinioid dinocyst species (Figure 8J) was originally reported in Burdigalian–Messinian deposits in the Gulf of Mexico as *Trinovantedinium* sp. (Duffield and Stein, 1986, Plate 2, Figures 10–11). Subsequently, De Verteuil and Norris (1996) formally described this species and proposed a lower Serravallian–Zanclean stratigraphic range, interpreting Burdigalian and Langhian occurrences in the Gulf of Mexico as caving. However, the continuous occurrence of *T. papula* in the lower part of WA suggest that the FAD of this species in the Colombian Caribbean Margin may extend at least to the Aquitanian (Figure 3, Figure 4).

5.3. PALEOPRODUCTIVITY

Differences in the P/G ratio (Figure 5), the abundance of foraminiferal test linings (Figure 5), and the multivariate analysis (Figure 6) indicate two distinct assemblages in WA. The first assemblage, 881–533 m (2890′–1750′), is strongly dominated by peridinioid dinocysts (mostly heterotrophic), whereas the second assemblage, 524–40 m (1720′–130′), is strongly dominated by gonyaulacoid dinocysts (mostly autotrophic) (Figure 5, Figure 6). The timing of the shift, 533–524 m (1750′–1720′) is near the Aquitanian–Burdigalian boundary (~20.7 Ma) at the top of the Achomosphaera alcicornu zone (Figure 3, Figure 5).

Did taphonomic processes produce this shift? A factor that affects peridinioid dinocyst abundance, and thus P/G values, is water-depth. Peridinioid taxa are more abundant in proximal environments compared to distal environments (e.g., Radi and de Vernal, 2004; Holzwarth et al., 2007; Pospelova and Pedersen, 2008; Verleye and Louwye, 2010). Therefore, an increase in the abundance of peridinioid dinocysts towards

the upper part of WA would be expected due to the progradational trend in WA sequence (Figure 2). However, WA presents the opposite pattern—peridinioids are more abundant in the lower interval (Figure 5). Thus, we can discard water-depth as a reason for the observed trend. A second factor that could affect P/G values is differential dinocyst preservation. Peridinioid dinocysts and foraminiferal test linings are among the most sensitive palynomorphs to aerobic degradation (Zonneveld et al., 2007; Mudie and Yanko-Hombach, 2019). High values of bottom-water oxygen concentration exponentially increase the degradation of peridinioids in relation to gonyaulacoids (Zonneveld et al., 2007). Therefore, it is expected that the Uitpa Formation, which accumulated in middle/outer shelf depositional environments, would have lower values of bottom-water oxygen than the Jimol Formation, which accumulated in inner shelf/shoreface depositional environments. Nevertheless, the shift in P/G values at ~529 m (~1735′) occurs within the Uitpa Formation and not at the Uitpa/Jimol boundary (~393 m; 1290′) (Figure 5). Thus, we also can discard differential dinocyst preservation as a viable factor.

Taphonomy, therefore, cannot explain either the shift in dinocyst communities or the drop in P/G values in WA. An alternative explanation that may explain both changes is a decrease in marine primary productivity in the Cocinetas Basin, which may have shifted the communities from high to low productivity and therefore increased the P/G ratio in the upper interval of WA. Was this reduction in paleoproductivity driven by terrestrial runoff or coastal upwelling? The P/G ratio alone cannot distinguish between both types of marine primary productivity (Sluijs et al., 2005). Instead, the analysis of terrestrial and marine palynomorphs can solve this dichotomy. High abundance of

terrestrially-derived palynomorphs will be expected if marine productivity is driven by fluvial runoff. For instance, terrestrial palynomorphs predominate in the Orinoco River plume region where productivity is modulated by river discharge (Muller, 1959), whereas marine palynomorphs predominate in the Cariaco Basin where productivity is modulated by coastal upwelling (Bringué et al., 2018, Bringué et al., 2019). In WA, a larger Terrestrial/Marine (T/M) index would be expected in the lower interval (881–533 m) in relation to the upper interval (524–40 m) if productivity was driven by terrestrial runoff. However, there are no significant differences between these two intervals (Figure 5). In addition, estimates of mean annual precipitation in the Cocinetas Basin show constant rainfall values (~2000 mm) throughout the early Miocene (~24–18 Ma) (Jaramillo et al., 2020). Thus, we can also discard terrestrial runoff as a viable factor in the shift from a peridinioid-dominated assemblage to a gonyaulacoid-dominated assemblage.

It is possible that the shift in WA assemblages was driven by a sharp decrease in upwelling at the Aquitanian–Burdigalian boundary (Figure 5). Coastal upwelling is not widespread in the modern southern Caribbean. When present, coastal upwelling is seasonal and restricted to the western margins of coastal landforms that protrude into the south-westward flow of the Caribbean Low-Level Jet (e.g., Guajira Peninsula, Margarita Island) (Andrade and Barton, 2005). This upwelling system is characterized by two strong upwelling periods of similar intensity during February–March (3.7 ± 1.6 m2 s−1) and June–July (3.5 ± 1.4 m2 s−1), and lower upwelling regimes during the remaining months (~2.1 ± 0.8 m2 s−1) (Rueda-Roa et al., 2018). The system is ultimately controlled by seasonal migration of the Intertropical Convergence Zone (ITCZ) and associated Trade Wind intensity. The southern position of the ITCZ during January–March

strengthens the Trade Winds, enhancing upwelling and reducing rainfall, whereas the northern position of the ITCZ during June–July weakens the Trade Winds, diminishing upwelling and increasing rainfall (Schneider et al., 2014). In addition, seasonal intensification of the Caribbean Current induces the mid-year upwelling (Muller-Karger et al., 2004; Rueda-Roa et al., 2018).

Miocene and modern oceanographic conditions in the circum-Caribbean differ. Paleogeographic reconstructions of the region indicate a narrow (~500 km) and deep (≥500 m) Central American Seaway (CAS) during the early Miocene (Duque-Caro, 1990; Montes et al., 2012; Farris et al., 2011; Sepulchre et al., 2014; Jaramillo, 2018). A sensitivity study that estimated CAS throughflow under comparable paleogeographic conditions (2700 m deep, 440 km wide, south-north oriented CAS at 8°N) yielded a net eastward flow through CAS (~7.6 × 106 m3 s−1), as a result of westward transport of proto-Caribbean shallow waters (~7.2 × 106 m3 s−1) and eastward transport of Pacific intermediate and deep waters (~14.8 × 106 m3 s−1) (Sepulchre et al., 2014) (Figure 10). This inflow of Pacific waters to the proto-Caribbean during the early Miocene, therefore, indicates that the proto-Caribbean was cooler, less saline and more productive than the modern Caribbean (Jaramillo, 2018 and references therein). Oceanographic simulations with analogous parameterization (2000 m deep, 450 km wide CAS with ~10.6–13.8 × 106 m3 s−1 CAS eastward throughflow) show similar simulated net primary production between the North Atlantic (3.3–5.2 Gt C yr−1) and the North Pacific (2.8–5.2 Gt C yr−1), supporting trans-equatorial transport of nutrients through CAS (Schneider and Schmittner, 2006). Likewise, upwelling along the northern coast of South America during the early Miocene, based on a marked contrast between the southernmost proto-

Caribbean (~19–20 °C) and the rest of the region (>21 °C), has also been proposed (von der Heydt and Dijkstra, 2005). Therefore, it seems possible to assume that the southern Caribbean had more productive waters during the early Miocene compared to modern Caribbean conditions, which may explain the higher productivity observed in the lower interval of WA (Figure 5).

What could have produced the permanent and abrupt productivity drop and dinocyst community shift near the Aquitanian–Burdigalian boundary (~20.7 Ma)? A first possibility is a permanent southward migration of the ITCZ, thus reducing coastal upwelling. However, empirical records for the Cocinetas Basin do not show major changes in precipitation during the early or middle Miocene (Scholz et al., 2020; Jaramillo et al., 2020). A second explanation is a local isolation of the Cocinetas Basin from the proto-Caribbean due to tectonic processes. However, there are high average subsidence rates (~120–360 m/m.y.; not decompacted) along the southwestern Caribbean pull-apart system (Guajira Peninsula, Falcón Basin, Urumaco Trough, Paraguaná Peninsula) during the early Miocene (Macellari, 1995). A third explanation is a permanent reduction of high-nutrient waters reaching the Cocinetas Basin. As most nutrient waters reaching the southern proto-Caribbean were sourced from deep and intermediate Pacific waters through CAS, a constriction of this source could have decreased nutrient availability in the southern Caribbean. Tectonic collision between the Panama microplate and the South American plate began at ~25 Ma, leading to extensive exhumation in the northern Andes and Panama (Farris et al., 2011), and consequently, constriction of CAS to ~200 km (Montes et al., 2012) (Figure 10). By ~21 Ma, an extensive terrestrial landscape in central Panama with well-established tropical

rainforests was already part of a continuous peninsula connecting Central and North America (Jaramillo, 2018) (Figure 10B). We hypothesize that this first major constriction of CAS produced a decrease in the rate and volume of Pacific waters delivered into the proto-Caribbean, thus driving the pattern in the Cocinetas Basin. This early Miocene permanent reduction in paleoproductivity along the Colombian Caribbean Margin requires further study. Paleoproductivity reconstructions have mostly focused on the late Miocene and Pliocene (e.g., Jain and Collins, 2007; Jain et al., 2007; O'Dea et al., 2007, O'Dea et al., 2012; Leigh et al., 2014; Grossman et al., 2019), whereas very few studies have been performed on the entire Neogene productivity record (e.g., Zegarra and Helenes, 2011). Furthermore, additional sensitivity modeling studies are required to fully understand the relationship between productivity, Trade Winds, the ITZC, and coastal geomorphology of the southern Caribbean and the tropical eastern Pacific regions.

Figure 10. Paleogeographic reconstruction during the late Oligocene and early Miocene, showing a reduction in the net inflow of Pacific deep and intermediate, nutrient-rich, waters into the proto-Caribbean in response to the constriction of the Central American Seaway (CAS) (modified from Bloch et al., 2016; Jaramillo, 2018). CAS throughflow based on Sepulchre et al. (2014).

6. CONCLUSIONS

A biostratigraphic scheme is proposed for the lower Miocene succession in the Cocinetas Basin, comprising an upper Chattian–lower Aquitanian *Minisphaeridium latirictum* Interval Zone (~23.9–22.0 Ma), an upper Aquitanian *Achomosphaera alcicornu* Interval Zone (~22.0–20.3 Ma), and a Burdigalian *Cribroperidinium tenuitabulatum* Interval Zone (~20.3–17.5 Ma).

A sudden shift in dinocyst communities (from peridinioid-dominated to gonyaulacoid-dominated) and the Peridinioid/Gonyaulacoid (P/G) ratio near the Aquitanian–Burdigalian boundary (~20.7 Ma) indicate a rapid and permanent drop in marine primary productivity in the Cocinetas Basin. This change cannot be explained by taphonomy, local tectonics, or changes in local precipitation and terrestrial runoff. Instead, this paleoproductivity reduction was likely the product of the initial constriction of the Central American Seaway during the early Miocene.

ACKNOWLEDGMENTS

We especially thank Lucy Edwards (USGS, Reston) and Stephen Louwye (Ghent University) for their invaluable help identifying palynomorphs, as well as Diego Pinzón (IANIGLA, CCT-CONICET Mendoza) for his biostratigraphic input. We also acknowledge the Colombian National Hydrocarbons Agency for providing access to the Well A samples. Sincere thanks to two anonymous reviewers for providing constructive comments that improved the quality of the manuscript. We are grateful to journal editor

Howard Falcon-Lang for handling the manuscript. Partial funding was provided by the Geological Society of America (GSA Graduate Student Research Grant) and the Paleontological Society (Yochelson Student Research Award).

APPENDIX

Supplementary material related to this article can be found online at https://doi.org/10.1016/j.palaeo.2020.109955

REFERENCES

Andrade, C.A., Barton, E.D., 2005. The Guajira upwelling system. Cont. Shelf Res. 25, 1003–1022. https://doi.org/10.1016/J.CSR.2004.12.012.

Bloch, J.I., Woodruff, E.D., Wood, A.R., Rincon, A.F., Harrington, A.R., Morgan, G.S., Foster, D.A., Montes, C., Jaramillo, C.A., Jud, N.A., Jones, D.S., MacFadden, B.J., 2016. First north American fossil monkey and early Miocene tropical biotic inter- change. Nature 533, 243–246. https://doi.org/10.1038/nature17415.

Boonstra, M., Ramos, M.I.F., Lammertsma, E.I., Antoine, P.-O., Hoorn, C., 2015. Marine connections of Amazonia: evidence from foraminifera and dinoflagellate cysts (early to middle Miocene, Colombia/Peru). Palaeogeogr. Palaeoclimatol. Palaeoecol. 417, 176–194. https://doi.org/10.1016/J.PALAEO.2014.10.032.

Boyd, J.L., Riding, J.B., Pound, M.J., De Schepper, S., Ivanovic, R.F., Haywood, A.M., Wood, S.E.L., 2018. The relationship between Neogene dinoflagellate cysts and global climate dynamics. Earth-Science Rev. 177, 366–385. https://doi.org/10.1016/J.EARSCIREV.2017.11.018.

Bringué, M., Thunell, R.C., Pospelova, V., Pinckney, J.L., Romero, O.E., Tappa, E.J., 2018.

Physico-chemical and biological factors influencing dinoflagellate cyst production in the Cariaco Basin. Biogeosciences 15, 2325–2348. https://doi.org/10.5194/bg-15-2325-2018.

Bringué, M., Pospelova, V., Tappa, E.J., Thunell, R.C., 2019. Dinoflagellate cyst production in the Cariaco Basin: a 12.5 year-long sediment trap study. Prog. Oceanogr. 171, 175–211. https://doi.org/10.1016/j.pocean.2018.12.007.

Bujak, J.P., Downie, C., Eaton, G.L., Williams, G.L., 1980. Dinoflagellate Cysts and Acritarachs from the Eocene of Southern England. Spec. Pap. Palaeontol. 24.

Carrillo-Briceño, J.D., Argyriou, T., Zapata, V., Kindlimann, R., Jaramillo, C., 2016. A New early Miocene (Aquitanian) Elasmobranchii Assemblage from the la Guajira Peninsula, Colombia. Ameghiniana 53, 77–99.

Clarke, K.R., 1993. Non-parametric multivariate analyses of changes in community structure. Aust. J. Ecol. 18, 117–143. https://doi.org/10.1111/j.1442-9993.1993.tb00438.x.

Collins, L.S., Coates, A.G., Berggren, W.A., Aubry, M.-P., Zhang, J., 1996. The late Miocene Panama isthmian strait. Geology 24, 687–690. https://doi.org/10.1130/0091-7613(1996)024<0687:TLMPIS>2.3.CO;2.

Colón, J.A., 1963. Seasonal variations in heat flux from the sea surface to the atmosphere over the Caribbean Sea. J. Geophys. Res. 68, 1421–1430. https://doi.org/10.1029/JZ068i005p01421.

Dalgaard, P., 2008. Introductory Statistics with R. Springer-Verlag New Yorkhttps://doi.org/10.1007/978-0-387-79054-1.

De Porta, J., 1974. Léxico Estratigráfico. Amerique Latine, Colombie (deuxiéme partie). Tertiaire et Quaternaire. Union Internationale des Sciences Geologiques, Paris.

De Schepper, S., Beck, K.M., Mangerud, G., 2017. Late Neogene dinoflagellate cyst and acritarch biostratigraphy for Ocean Drilling Program Hole 642B, Norwegian Sea. Rev. Palaeobot. Palynol. 236, 12–32. https://doi.org/10.1016/J.REVPALBO.2016.08.005.

De Verteuil, L., 1996. Data Report: Upper Cenozoic Dinoflagellate Cysts from the Continental Slope and Rise off New Jersey, in: Mountain, G.S., Miller, K.G., Blum, P., Poag, C.W., Twichell, D.C. (Eds.), Proceedings of the Ocean Drilling Program, Scientific Results Volume 150. pp. 439–454.

De Verteuil, L., Norris, G., 1992. Miocene Protoperidiniacean Dinoflagellate Cysts from the Maryland and Virginia Coastal Plain, in: Head, M.J., Wrenn, J.H. (Eds.), Neogene and Quaternary Dinoflagellate Cysts and Acritarchs. American Asociation of Stratigraphic Palynologists Foundation, pp. 391–430.

De Verteuil, L., Norris, G., 1996. Miocene Dinoflagellate Stratigraphy and Systematics of Maryland and Virginia. Micropaleontology 42, 1–172. https://doi.org/10.2307/1485926.

Duffield, S.L., Stein, J.A., 1986. Peridiniacean-dominated dinoflagellate cyst assemblages from the Miocene of the Gulf of Mexico shelf, offshore Louisiana. In: Wrenn, J.H., Duffield, Susan L., Stein, Jeffrey A. (Eds.), Papers from the First Symposium on Neogene Dinoflagellate Cyst Biostratigraphy. vol. 17. pp. 27–45 American Asociation of Stratigraphic Palynologists Contribution Series No.

Duque-Caro, H., 1990. Neogene stratigraphy, paleoceanography and paleobiogeography in Northwest South America and the evolution of the Panama seaway. Palaeogeogr. Palaeoclimatol. Palaeoecol. 77, 203–234. https://doi.org/10.1016/0031-0182(90) 90178-A.

Duque-Herrera, A.-F., Helenes, J., Pardo-Trujillo, A., Flores-Villarejo, J.-A., Sierro-Sánchez, F.-J., 2018. Miocene biostratigraphy and paleoecology from dinoflagellates, benthic foraminifera and calcareous nannofossils on the Colombian Pacific coast. Mar. Micropaleontol. 141, 42–54. https://doi.org/10.1016/J.MARMICRO.2018.05. 002.

Dybkjær, K., Piasecki, S., 2010. Neogene dinocyst zonation for the eastern North Sea Basin, Denmark. Rev. Palaeobot. Palynol. 161, 1–29. https://doi.org/10.1016/J.REVPALBO.2010.02.005.

Edwards, L.E., Weems, R.E., Carter, M.W., Spears, D.B., Powars, D.S., 2018. The significance of dinoflagellates in the Miocene Choptank Formation beneath the Midlothian gravels in the southeastern Virginia Piedmont. Stratigraphy 15, 179–195. https://doi.org/10.29041/strat.15.179-195.

Farris, D.W., Jaramillo, C., Cardona, A., Montes, C., Bayona, G., Restrepo-Moreno, S.A., Mora, A., Speakman, R.J., Glascock, M.D., Valencia, V., 2011. Fracturing of the Panamanian Isthmus during initial collision with South America. Geology 39, 1007–1010. https://doi.org/10.1130/G32237.1.

Fensome, R.A., Williams, G.L., MacRae, R.A., 2009. Late Cretaceous and Cenozoic fossil dinoflagellates and other palynomorphs from the scotian margin, offshore eastern Canada. J. Syst. Palaeontol. 7, 1–79. https://doi.org/10.1017/S1477201908002538.

Fensome, R.A., Nøhr-Hansen, H., Williams, G.L., 2016. Cretaceous and Cenozoic dinoflagellate cysts and other palynomorphs from the western and eastern margins of the Labrador–Baffin Seaway. Geol. Surv. Denmark and Greenland Bull. 36.

Fensome, R.A., Williams, G.L., MacRae, R.A., 2019. The Lentin and Williams Index of Fossil Dinoflagellates. American Association of Stratigraphic Palynologists Foundation (Contribution Series 50).

Gordon, A., 1966. Caribbean Sea–Oceanography. In: Fairbridge, R.W. (Ed.), Encyclopedia of Oceanography. Reinhold, pp. 175–181 New York.

Groeneveld, J., Nürnberg, D., Tiedemann, R., Reichart, G.-J., Steph, S., Reuning, L., Crudeli, D., Mason, P., 2008. Foraminiferal Mg/Ca increase in the Caribbean during the Pliocene: Western Atlantic Warm Pool formation, salinity influence, or diagenetic overprint? Geochem. Geophys. Geosyst. 9. https://doi.org/10.1029/2006GC001564.

Grøsfjeld, K., Dybkjær, K., Eidvin, T., Riis, F., Rasmussen, E., Knies, J., 2019. A Miocene age for the Molo Formation, Norwegian Sea shelf off Vestfjorden, based on marine palynology. Nor. J. Geol. 99, 1–25.

Grossman, E.L., Robbins, J.A., Rachello-Dolmen, P.G., Tao, K., Saxena, D., O'Dea, A., 2019. Freshwater input, upwelling, and the evolution of Caribbean coastal ecosystems during formation of the Isthmus of Panama. Geology 47, 857–861. https://doi. org/10.1130/G46357.1.

Gussone, N., Eisenhauer, A., Tiedemann, R., Haug, G.H., Heuser, A., Bock, B., Nägler, T.F., Müller, A., 2004. Reconstruction of Caribbean Sea surface temperature and salinity fluctuations in response to the Pliocene closure of the Central American Gateway and radiative forcing, using δ44/40Ca, δ18O and Mg/Ca ratios. Earth Planet. Sci. Lett. 227, 201–214. https://doi.org/10.1016/J.EPSL.2004.09.004.

Haug, G.H., Tiedemann, R., 1998. Effect of the formation of the Isthmus of Panama on Atlantic Ocean thermohaline circulation. Nature 393, 673–676. https://doi.org/10.1038/31447.

Haug, G.H., Tiedemann, R., Zahn, R., Ravelo, A.C., 2001. Role of Panama uplift on oceanic freshwater balance. Geology 29, 207–210. https://doi.org/10.1130/0091-7613(2001)029<0207:ROPUOO>2.0.CO;2.

Helenes, J., Cabrera, D., 2003. Oligocene-Miocene palynomorph assemblages from eastern Venezuela. Palynology 27, 5–25. https://doi.org/10.1080/01916122.2003.9989579.

Hendy, A.J.W., Jones, D.S., Moreno, F., Zapata, V., Jaramillo, C., 2015. Neogene molluscs, shallow marine paleoenvironments, and chronostratigraphy of the Guajira Peninsula, Colombia. Swiss J. Palaeontol. 134, 45–75. https://doi.org/10.1007/s13358-015-0074-1.

von der Heydt, A., Dijkstra, H.A., 2005. Flow reorganizations in the Panama Seaway: a cause for the demise of Miocene corals? Geophys. Res. Lett. 32. https://doi.org/10. 1029/2004GL020990.

Holzwarth, U., Esper, O., Zonneveld, K., 2007. Distribution of organic-walled dinoflagellate cysts in shelf surface sediments of the Benguela upwelling system in relationship to environmental conditions. Mar. Micropaleontol. 64, 91–119. https:// doi.org/10.1016/J.MARMICRO.2007.04.001.

Hoorn, C., 1993. Marine incursions and the influence of Andean tectonics on the Miocene depositional history of northwestern Amazonia: results of a palynostratigraphic study. Palaeogeogr. Palaeoclimatol. Palaeoecol. 105, 267–309. https://doi.org/10. 1016/0031-0182(93)90087-Y.

Hoorn, C., 1994. An environmental reconstruction of the palaeo-Amazon River system (Middle–late Miocene, NW Amazonia). Palaeogeogr. Palaeoclimatol. Palaeoecol. 112, 187–238. https://doi.org/10.1016/0031-0182(94)90074-4.

Jain, S., Collins, L.S., 2007. Trends in Caribbean Paleoproductivity related to the Neogene closure of the Central American Seaway. Mar. Micropaleontol. 63, 57–74. https://doi.org/10.1016/J.MARMICRO.2006.11.003.

Jain, S., Collins, L.S., Hayek, L.-A.C., 2007. Relationship of benthic foraminiferal diversity to paleoproductivity in the Neogene Caribbean. Palaeogeogr. Palaeoclimatol. Palaeoecol. 255, 223–245. https://doi.org/10.1016/J.PALAEO.2007.05.017.

Jaramillo, C., Romero, I., D'Apolito, C., Bayona, G., Duarte, E., Louwye, S., Escobar, J., Luque, J., Carrillo-Briceño, J.D., Zapata, V., Mora, A., Schouten, S., Zavada, M., Harrington, G., Ortiz, J., Wesselingh, F.P., 2017. Miocene flooding events of western Amazonia. Sci. Adv. 3, e1601693. https://doi.org/10.1126/sciadv.1601693.

Jaramillo, C., Sepulchre, P., Cárdenas, D., Correa-Metrio, A., Moreno, J.E., Trejos, R., Vallejos, D., Hoyos, N., Martínez, C., Carvalho, D., Escobar, J., Oboh-Ikuenobe, F., Prámparo, M.B., Pinzón, D., 2020. Drastic vegetation change in the Guajira Peninsula (Colombia) during the Neogene. Paleoceanogr. Paleoclimatology 35, e2020PA003933. https://doi.org/10.1029/2020PA003933.

Jaramillo, C.A., 2018. Evolution of the Isthmus of Panama: Biological, Paleoceanographic and Paleoclimatological Implications. In: Carina, H., Allison, P., Alexandre, A. (Eds.), Mountains, Climate and Biodiversity. John Wiley & Sons, Hoboken, New Jersey, pp. 323–338.

Jaramillo, C.A., Rueda, M., Torres, V., 2011. A palynological zonation for the Cenozoic of the Llanos and Llanos Foothills of Colombia. Palynology 35, 46–84. https://doi.org/ 10.1080/01916122.2010.515069.

Johns, W.E., Townsend, T.L., Fratantoni, D.M., Wilson, W.D., 2002. On the Atlantic inflow to the Caribbean Sea. Deep Sea Res. Part I Oceanogr. Res. Pap. 49, 211–243. https://doi.org/10.1016/S0967-0637(01)00041-3.

Keigwin, L., 1982. Isotopic Paleoceanography of the Caribbean and East Pacific: Role of Panama Uplift in late Neogene Time. Science. https://doi.org/10.1126/science.217. 4557.350. (80-.). 217, 350 LP – 353.

Kruskal, J.B., 1964. Nonmetric multidimensional scaling: a numerical method. Psychometrika 29, 115–129. https://doi.org/10.1007/BF02289694.

Lammertsma, E.I., Troelstra, S.R., Flores, J.-A., Sangiorgi, F., Chemale Jr., F., do Carmo, D.A., Hoorn, C., 2018. Primary productivity in the western tropical Atlantic follows Neogene Amazon River evolution. Palaeogeogr. Palaeoclimatol. Palaeoecol. 506, 12–21. doi:https://doi.org/10.1016/J.PALAEO.2018.05.048.

Leigh, E.G., O'Dea, A., Vermeij, G.J., 2014. Historical biogeography of the Isthmus of Panama. Biol. Rev. 89, 148–172. https://doi.org/10.1111/brv.12048.

LeNoir, E.A., Hart, G.F., 1986. Burdigalian (early Miocene) dinocysts from offshore Louisiana. In: Wrenn, J.H., Duffield, S.L., Stein, J.A. (Eds.), Papers from the First Symposium on Neogene Dinoflagellate Cyst Biostratigraphy. vol. 17. pp. 59–81 American Asociation of Stratigraphic Palynologists Contribution Series No.

Louwye, S., Foubert, A., Mertens, K., Van Rooij, D., 2008. Integrated stratigraphy and palaeoecology of the lower and middle Miocene of the Porcupine Basin. Geol. Mag. 145, 321–344. https://doi.org/10.1017/S0016756807004244.

Macellari, C.E., 1995. In: Tankard, A.J., Soruco, R.S., Welsink, H.J. (Eds.), Cenozoic Sedimentation and Tectonics of the Southwestern Caribbean Pull-Apart Basin, Venezuela and Colombia. American Association of Petroleum Geologists, pp. 757–780. https://doi.org/10.1306/M62593C41. Petroleum Basins of South America.

Montes, C., Cardona, A., McFadden, R., Morón, S.E., Silva, C.A., Restrepo-Moreno, S., Ramírez, D.A., Hoyos, N., Wilson, J., Farris, D., Bayona, G.A., Jaramillo, C.A., Valencia, V., Bryan, J., Flores, J.A., 2012. Evidence for middle Eocene and younger land emergence in Central Panama: Implications for Isthmus closure. GSA Bull. 124, 780–799. https://doi.org/10.1130/B30528.1.

Moreno, F., Hendy, A.J.W., Quiroz, L., Hoyos, N., Jones, D.S., Zapata, V., Zapata, S., Ballen, G.A., Cadena, E., Cárdenas, A.L., Carrillo-Briceño, J.D., Carrillo, J.D., Delgado-Sierra, D., Escobar, J., Martínez, J.I., Martínez, C., Montes, C., Moreno, J., Pérez, N., Sánchez, R., Suárez, C., Vallejo-Pareja, M.C., Jaramillo, C., 2015. Revised stratigraphy of Neogene strata in the Cocinetas Basin, La Guajira, Colombia. Swiss J. Palaeontol. 134, 5–43. https://doi.org/10.1007/s13358-015-0071-4.

Mudie, P.J., Yanko-Hombach, V., 2019. Microforaminiferal linings as proxies for paleosalinity and pollution: Danube Delta example. Micropaleontology 65, 27–45.

Muller, J., 1959. Palynology of recent Orinoco delta and shelf sediments; reports of the Orinoco shelf expedition, volume 5. Micropaleontology 5, 1–32.

Muller-Karger, F., Varela, R., Thunell, R., Astor, Y., Zhang, H., Luerssen, R., Hu, C., 2004. Processes of coastal upwelling and carbon flux in the Cariaco Basin. Deep Sea Res. Part II Top. Stud. Oceanogr. 51, 927–943. https://doi.org/10.1016/J.DSR2.2003.10. 010.

Müller-Karger, F.E., McClain, C.R., Fisher, T.R., Esaias, W.E., Varela, R., 1989. Pigment distribution in the Caribbean Sea: Observations from space. Prog. Oceanogr. 23, 23–64. https://doi.org/10.1016/0079-6611(89)90024-4.

Munsterman, D.K., Brinkhuis, H., 2004. A southern North Sea Miocene dinoflagellate cyst zonation. Netherlands J. Geosci. - Geol. en Mijnb. 83, 267–285. https://doi.org/10. 1017/S0016774600020369.

O'Dea, A., Jackson, J.B.C., Fortunato, H., Smith, J.T., D'Croz, L., Johnson, K.G., Todd, J.A., 2007. Environmental change preceded Caribbean extinction by 2 million years. Proc. Natl. Acad. Sci. 104, 5501 LP–5506. https://doi.org/10.1073/pnas.0610947104.

O'Dea, A., Hoyos, N., Rodríguez, F., Degracia, B., De Gracia, C., 2012. History of upwelling in the Tropical Eastern Pacific and the paleogeography of the Isthmus of Panama. Palaeogeogr. Palaeoclimatol. Palaeoecol. 348–349, 59–66. https://doi.org/ 10.1016/J.PALAEO.2012.06.007.

Oksanen, J., Blanchet, F.G., Friendly, M., Kindt, R., Legendre, P., McGlinn, D., Minchin, P. R., O'Hara, R.B., Simpson, G.L., Solymos, P., Szoecs, M.H.H.S.E., Wagner, H., 2019. vegan: Community ecology package.

Ortiz, J.R., Jaramillo, C., Moreno, C., 2019. SDAR: A Toolkit for Stratigraphic Data Analysis in R.

Parra, F.J., Navarrete, R.E., di Pasquo, M.M., Roddaz, M., Calderón, Y., Baby, P., 2019. Neogene palynostratigraphic zonation of the Maranon Basin, Western Amazonia, Peru. Palynology 1–21. https://doi.org/10.1080/01916122.2019.1674395.

Pérez-Consuegra, N., Góngora, D.E., Herrera, F., Jaramillo, C., Montes, C., Cuervo-Gómez, A.M., Hendy, A., Machado, A., Cárdenas, D., Bayona, G., 2018. New records of Humiriaceae fossil fruits from the Oligocene and early Miocene of the western Azuero Peninsula, Panamá. Bol. Soc. Geol. Mex. 70, 223–239.

Pospelova, V., Pedersen, T.F., 2008. Distribution of dinoflagellate cysts in surface sediments from the northeastern Pacific Ocean (43–25°N) in relation to sea-surface temperature, salinity, productivity and coastal upwelling. Mar. Micropaleontol. 68, 21–48. https://doi.org/10.1016/J.MARMICRO.2008.01.008.

Powell, A.J., Lewis, J., Dodge, J.D., 1992. The palynological expressions of post-Palaeogene upwelling: a review. Geol. Soc. Lond. Spec. Publ. 64, 215 LP–226. https://doi.org/10.1144/GSL.SP.1992.064.01.14.

R Core Team, 2017. R: A Language and Environment for Statistical Computing. R Foundation for Statistical Computing, Vienna, Austria URL. https://www.R-project. org/.

Radi, T., de Vernal, A., 2004. Dinocyst distribution in surface sediments from the northeastern Pacific margin (40–60°N) in relation to hydrographic conditions, pro- ductivity and upwelling. Rev. Palaeobot. Palynol. 128, 169–193. https://doi.org/10. 1016/S0034-6667(03)00118-0.

Renz, O., 1960. Geología de la parte sureste de la peninsula de La Guajira. III Congr. Geológico Venez. Boletín Geol. Publicación Espec. Minist. Minas e Hidrocarburos 3, 317–347.

Rollins, J.F., 1965. Stratigraphy and structure of the Goajira Peninsula, northwestern Venezuela and northeastern Colombia. Univ. Nebraska Stud. 30, 1–102.

Rueda-Roa, D.T., Ezer, T., Muller-Karger, F.E., 2018. Description and Mechanisms of the Mid-Year Upwelling in the Southern Caribbean Sea from Remote Sensing and Local Data. J. Mar. Sci. Eng. 6, 1–19.

Schneider, B., Schmittner, A., 2006. Simulating the impact of the Panamanian seaway closure on ocean circulation, marine productivity and nutrient cycling. Earth Planet. Sci. Lett. 246, 367–380. https://doi.org/10.1016/J.EPSL.2006.04.028.

Schneider, T., Bischoff, T., Haug, G.H., 2014. Migrations and dynamics of the intertropical convergence zone. Nature 513, 45–53. https://doi.org/10.1038/nature13636.

Scholz, S.R., Petersen, S.V., Escobar, J., Jaramillo, C., Hendy, A.J.W., Allmon, W.D., Curtis, J.H., Anderson, B.M., Hoyos, N., Restrepo, J.C., Perez, N., 2020. Isotope sclerochronology indicates enhanced seasonal precipitation in northern South America (Colombia) during the Mid-Miocene Climatic Optimum. Geology 48, 668–672. https://doi.org/10.1130/G47235.1.

Schreck, M., Matthiessen, J., Head, M.J., 2012. A magnetostratigraphic calibration of Middle Miocene through Pliocene dinoflagellate cyst and acritarch events in the Iceland Sea (Ocean Drilling Program Hole 907A). Rev. Palaeobot. Palynol. 187, 66–94. https://doi.org/10.1016/J.REVPALBO.2012.08.006.

Schreck, M., Nam, S.-I., Clotten, C., Fahl, K., De Schepper, S., Forwick, M., Matthiessen, J., 2017. Neogene dinoflagellate cysts and acritarchs from the high northern latitudes and their relation to sea surface temperature. Mar. Micropaleontol. 136, 51–65. https://doi.org/10.1016/J.MARMICRO.2017.09.003.

Sepulchre, P., Arsouze, T., Donnadieu, Y., Dutay, J.-C., Jaramillo, C., Le Bras, J., Martin, E., Montes, C., Waite, A.J., 2014. Consequences of shoaling of the Central American Seaway determined from modeling Nd isotopes. Paleoceanography 29, 176–189. https://doi.org/10.1002/2013PA002501.

da Silva-Caminha, S.A.F., D'Apolito, C., Jaramillo, C., Espinosa, B.S., Rueda, M., 2020. Palynostratigraphy of the Ramon and Solimões formations in the Acre Basin, Brazil. J. S. Am. Earth Sci. 103, 102720. https://doi.org/10.1016/j.jsames.2020.102720.

Simpson, G.L., Oksanen, J., 2020. Analogue: Analogue and Weighted Averaging Methods for Palaeoecology.

Sluijs, A., Pross, J., Brinkhuis, H., 2005. From greenhouse to icehouse; organic-walled dinoflagellate cysts as paleoenvironmental indicators in the Paleogene. Earth-Science Rev. 68, 281–315. https://doi.org/10.1016/J.EARSCIREV.2004.06.001.

Soliman, A., Ćorić, S., Head, M.J., Piller, W.E., El Beialy, S.Y., 2012. Lower and Middle Miocene biostratigraphy, Gulf of Suez, Egypt based on dinoflagellate cysts and calcareous nannofossils. Palynology 36, 38–79. https://doi.org/10.1080/01916122.2011.633632.

Steph, S., Tiedemann, R., Groeneveld, J., Sturm, A., Nürnberg, D., 2006. Pliocene changes in Tropical East Pacific Upper Ocean Stratification: Response to Tropical Gateways? In: Tiedemann, R., Mix, A.C., Richter, C., Ruddiman, W.F. (Eds.), Proceedings of the Ocean Drilling Program, Scientific Results. vol. 202. pp. 1–51.

Verleye, T.J., Louwye, S., 2010. Recent geographical distribution of organic-walled dinoflagellate cysts in the Southeast Pacific (25–53°S) and their relation to the pre- vailing hydrographical conditions. Palaeogeogr. Palaeoclimatol. Palaeoecol. 298, 319–340. https://doi.org/10.1016/J.PALAEO.2010.10.006.

Versteegh, G.J.M., 1994. Recognition of cyclic and non-cyclic environmental changes in the Mediterranean Pliocene: a palynological approach. Mar. Micropaleontol. 23, 147–183. https://doi.org/10.1016/0377-8398(94)90005-1.

Williams, G.L., Brinkhuis, H., Pearce, M.A., Fensome, R.A., Weegink, J.W., 2004. Southern Ocean and global dinoflagellate cyst events compared: Index events for the Late Cretaceous–Neogene. In: Exon, N.F., Kennett, J.P., Malone, M.J. (Eds.), Proceedings of the Ocean Drilling Program, Scientific Results. vol. 189. pp. 1–98.

Willumsen, P.S., Dale, B., Jolley, D.W., Laursen, G.V., 2014. Palynostratigraphy and palaeoenvironmental shifts in Oligocene and Miocene strata from offshore Angola, west-central Africa. Palynology 38, 259–279. https://doi.org/10.1080/01916122.2014.886630.

Wood, G.D., Gabriel, A.M., Lawson, J.C., 1996. Palynological techniques – Processing and microscopy. In: Jansonius, J., McGregor, D.C. (Eds.), Palynology: Principles and Applications. vol. 1. Dallas, Texas, pp. 29–50 AASP – The Palynological Society.

Zegarra, M., Helenes, J., 2011. Changes in Miocene through Pleistocene dinoflagellates from the Eastern Equatorial Pacific (ODP Site 1039), in relation to primary productivity. Mar. Micropaleontol. 81, 107–121. https://doi.org/10.1016/J.MARMICRO.2011.09.005.

Zevenboom, D., 1995. Dinoflagellate Cysts from the Mediterranean Late Oligocene and Miocene. Utrecht University.

Zonneveld, K.A.F., Bockelmann, F., Holzwarth, U., 2007. Selective preservation of organic-walled dinoflagellate cysts as a tool to quantify past net primary production and bottom water oxygen concentrations. Mar. Geol. 237, 109–126. https://doi.org/ 10.1016/J.MARGEO.2006.10.023.

Zwiep, K.L., Hennekam, R., Donders, T.H., van Helmond, N.A.G.M., de Lange, G.J., Sangiorgi, F., 2018. Marine productivity, water column processes and seafloor anoxia in relation to Nile discharge during sapropels S1 and S3. Quat. Sci. Rev. 200, 178–190. https://doi.org/10.1016/J.QUASCIREV.2018.08.026.

II. NEW ACRITARCH AND PERIDINIOID DINOFLAGELLATE CYSTS SPECIES FROM THE OLIGOCENE–MIOCENE OF COLOMBIA

Damián Cárdenas, Francisca Oboh-Ikuenobe, Carlos Jaramillo

Department of Geosciences and Geological and Petroleum Engineering, Missouri University of Science and Technology, Rolla, MO 65409

ABSTRACT

New marine palynomorph taxa recovered from an upper Oligocene–lower Miocene (upper Chattian–upper Burdigalian; ~24–17 Ma) shallow-marine succession drilled in northern Colombia, northwestern South America, are herein formally described. These new taxa comprise two peridinioid dinoflagellate cyst species, *Cristadinium lucyae* sp. nov., and *Trinovantedinium uitpensis* sp. nov., and the acritarch *Quadrina*? *triangulata* sp. nov.. During the Aquitanian, *C. lucyae* sp. nov. occurs consistently, whereas *T. uitpensis* sp. nov. occurs sporadically. *Q.*? *triangulata* sp. nov., a potential key biostratigraphic marker in the tropical Americas, occurs during the middle and upper Burdigalian. *Cristadinium lucyae* sp. nov. is characterized by having solid, distally tapered to truncated, sutural spinules forming linear low crests. *Quadrina*? *triangulata* sp. nov. is characterized by having conical to subconical processes. *Trinovantedinium uitpensis* sp. nov. is characterized by having verrucate to slightly baculate penitabular processes and denticulate cingulum. In addition, *Cristadinium lucyae* sp. nov. and *Trinovantedinium uitpensis* sp. nov. improve our understanding of protoperidiniacean taxonomic diversity.

1. INTRODUCTION

Organic-walled marine palynomorphs (dinoflagellate cysts and acritarchs) are useful tools for biostratigraphic and paleoenvironmental analysis of neritic records. In spite of their importance, marine palynomorphs have been seldom studied in northwestern South America. A recent palynological study of an upper Chattian–upper Burdigalian shallow-marine succession drilled in the Guajira Peninsula (Well A) (Cárdenas et al., 2020), yielded several undescribed taxa. Herein, we formally describe two new peridinioid dinoflagellate cysts taxa, *Cristadinium lucyae* sp. nov. and *Trinovantedinium uitpensis* sp. nov., and one acritarch species, *Quadrina*? *triangulata* sp. nov.. *Cristadinium lucyae* sp. nov. was previously reported as *Cristadinium*? sp. in the Serravallian of the western North Atlantic (de Verteuil and Norris, 1992; Edwards et al., 2018). *Quadrina*? *triangulata* sp. nov. was previously reported as both Dinocyst XI in upper Burdigalian deposits from the Gulf of Mexico (LeNoir and Hart, 1986) and *Quadrina* "incerta" from the middle Burdigalian of northwestern South America (Jaramillo et al., 2017, 2020; Cárdenas et al., 2020). *Trinovantedinium uitpensis* sp. nov. was previously reported as *Trinovantedinium* sp. from Aquitanian deposits of northwestern South America (Cárdenas et al., 2020).

2. STRATIGRAPHIC FRAMEWORK

Since the middle to late Eocene, the east-west displacement between the Caribbean and South American tectonic plates developed a pull-apart system along the

northwestern margin of South America that reached subsidence rates (not decompacted) up to 360 m/m.y. and 190 m/m.y. during the Miocene and Pliocene, respectively (Macellari, 1995). Among the pull-apart basins, namely the northern Guajira Peninsula, Falcón Basin, Urumaco Trough, Paraguaná Peninsula, and Aruba offshore, the Cocinetas Basin in the northern Guajira Peninsula (Figure 1) has been the focus of extensive stratigraphic (Moreno et al., 2015) and paleontological work (Jaramillo et al., 2015, 2020, and references therein) over the last decade.

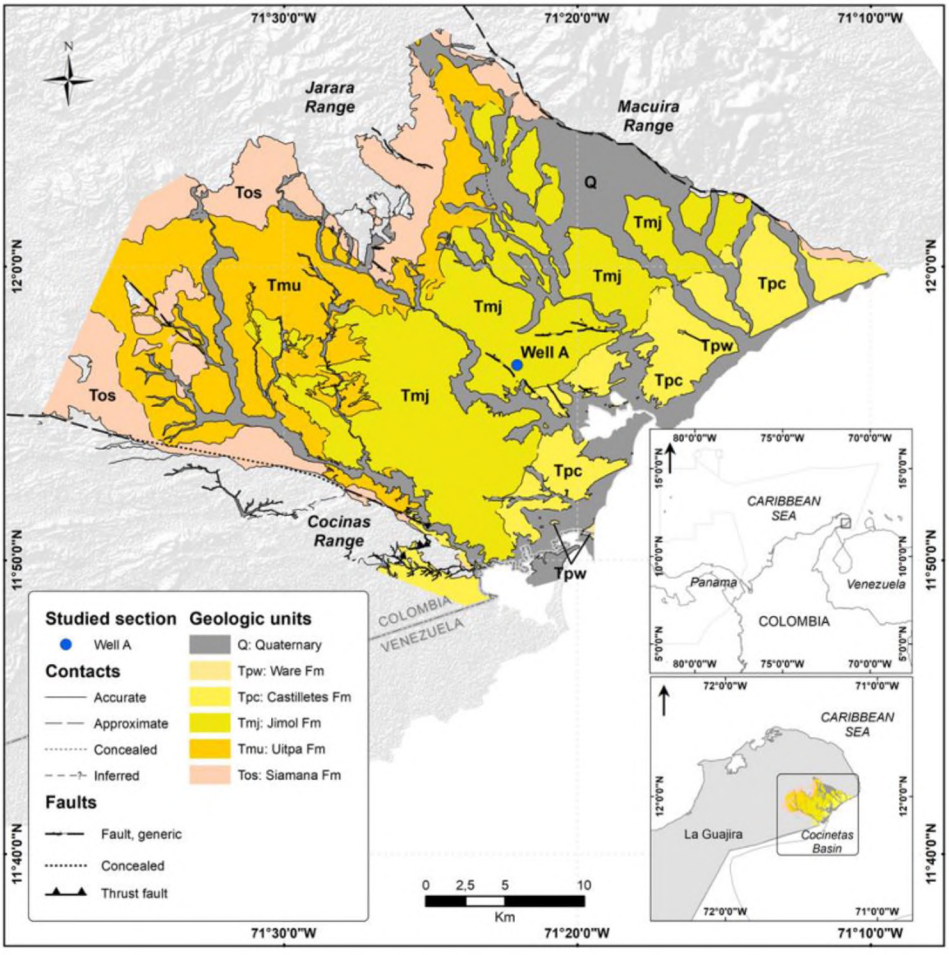

Figure 1. Geologic map of the Cocinetas Basin in northern Colombia, northwestern South America, showing the geographic location of the studied section (11°56'38''N, 71°22'03''W).

The Neogene sedimentary record of this basin comprises: (1) middle and outer shelf deposits (100–200 m water-depth) of the uppermost Oligocene–lower Burdigalian Uitpa Formation (~24.2–19.4 Ma) (Hendy et al., 2015; Carrillo-Briceño et al., 2016, Jaramillo et al., 2020); (2) shoreface and inner shelf deposits (<50 m water-depth) of the lower to upper Burdigalian Jimol Formation (~19.4–16.7 Ma) (Moreno et al., 2015, Jaramillo et al., 2020); (3) estuarine, lagoonal, shallow subtidal and fluvio-deltaic deposits of the upper Burdigalian–upper Langhian Castilletes Formation (~16.7–14.2 Ma) (Moreno et al., 2015); and (4) fluvio-deltaic deposits of the Piacenzian Ware Formation (~3.5–2.8 Ma) (Moreno et al., 2015) (Figure 1).

3. MATERIAL AND METHODS

Forty cuttings samples from a high-resolution, well-calibrated, shallow-marine succession drilled in the northern Guajira Peninsula (Well A), the northernmost geographic feature of South America, were recently analyzed for palynology (Cárdenas et al., 2020; Jaramillo et al., 2020). This sequence comprises ~900 m of interbedded sandstone, mudstone, limestone, siltstone and minor coal spanning the latest Oligocene and early Miocene (~24.1–17.3 Ma) with a sampling resolution of ~0.2 Ma (Figures 2–3). Calibration relied on calcareous nannoplankton, palynology, planktonic foraminifera, and Sr-isotope chronostratigraphy (Jaramillo et al., 2020). Acid-based palynological preparation was used to remove carbonates (HCl) and silicates (HF) in ~15–20 g per sample (Wood et al., 1996). Residues were sieved between 250 µm and 10 µm meshes, cleaned with brief ultrasonic treatment (~ 5–10 seconds), concentrated by centrifugation

(~ 7–15 minutes), mounted on a cover slide using polyvinyl alcohol solution and sealed using Canada balsam.

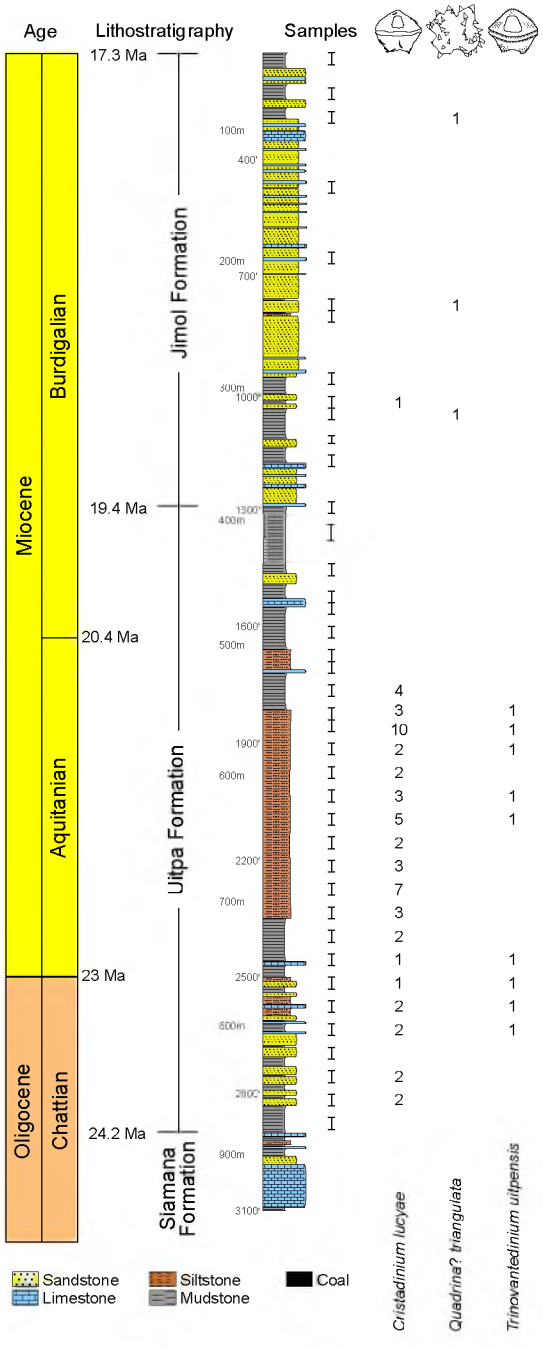

Figure 2. Lithostratigraphy of Well A showing the stratigraphic distribution of the palynological samples and the occurrences of the new marine palynomorph taxa.

Preservation of dinoflagellate cysts is moderate to excellent. A detailed record of all recovered marine palynomorphs can be found in Cárdenas et al. (2020). Photomicrographs were taken using a Nikon Eclipse 50iPOL microscope coupled to a DS-Fi3 camera. Dinoflagellate cyst taxonomic nomenclature follows the Lentin and Williams Index of fossil dinoflagellates (Fensome et al., 2019), whereas the suprageneric classification follows Fensome et al. (2013). Morphological terminology follows Evitt (1978) and Williams et al. (2000). We also follow the International Code of Nomenclature for algae, fungi, and plants (Turland et al., 2018). Holotypes and paratypes are housed at the palynological collection of the Instituto de Investigaciones en Estratigrafía (IIES), Universidad de Caldas, Manizales, Colombia (http://iies.edu.co/).

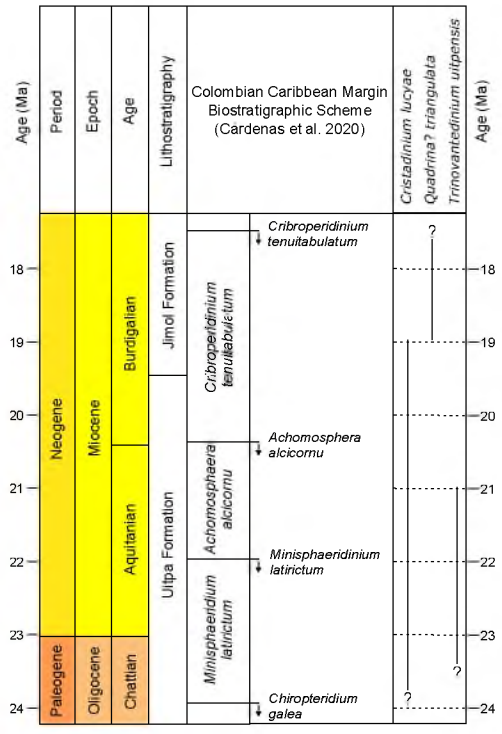

Figure 3. Range chart illustrating the stratigraphic distribution of the new marine palynomorph taxa in relation to the palynostratigraphic zones for the Colombian Caribbean Margin.

4. SYSTEMATIC PALEONTOLOGY

Division: DINOFLAGELLATA (Bütschli 1885) Fensome et al. 1993

Subdivision: DINOKARYOTA Fensome et al. 1993

Class: DINOPHYCEAE Pascher 1914

Subclass: PERIDINIPHYCIDAE Fensome et al. 1993

Order: PERDINIALES Haeckel 1894

Suborder: PERIDINIINEAE (Autonym)

Family: PROTOPERIDINIACEAE Balech 1988

Subfamily: PROTOPERIDINIOIDEAE Balech 1988

Genus: ***Cristadinium*** Head et al. 1989b emended Uddandam et al. 2018

Type species: *Cristadinium cristatoserratum* Head et al. 1989b

Species: *Cristadinium lucyae* sp. nov.

Figure 6, 1–16

Cristadinium? sp., de Verteuil and Norris 1992, Figure 7, 9–12; Edwards et al. 2018, Figure 5.4

Cristadinium sp., Jaramillo et al. 2020, Figure 5E; Cárdenas et al. 2020, Figures 7D, 7E

Etymology: Named after Dr. Lucy Edwards who has made fundamental contributions to the stratigraphy and marine palynology of the Atlantic and Gulf coastal plains.

Locality: Cocinetas Basin, La Guajira, Colombia.

Holotype: Figure 6, 1–4, Slide STRI 42198, Sample Well A 2020'–2050', England Finder reference K48/4.

Repository: Instituto de Investigaciones en Estratigrafía, Universidad de Caldas, Colombia. Catalogue number UC-B214-IIES-D-044-055.

Stratigraphic horizon: Uitpa Formation.

Age: Aquitanian, early Miocene.

Diagnosis: Peridinioid cyst weakly dorsoventrally compressed, proximate, acavate. Outline pentagonal in dorsoventral view, straight to slightly convex epicyst with reduced apical horn, straight to slightly concave hypocyst with two small antapical horns. Autophragm smooth with scattered solid ornamentation forming interrupted low sutural crests. Spinules tapered to truncated. Cingulum planar to slightly helicoidal bearing continuous crests along the anterior margin. Archeopyle intercalary hexa 2a, presumably isodeltalinteloid. Operculum free to adherent.

Description: Peridinioid cyst proximate, acavate and weakly dorsoventrally compressed with pentagonal outline in dorsoventral view: sides of the epicyst are straight to slightly convex, whereas sides of the hypocyst are straight to slightly concave; length of the epicyst and the hypocyst are approximately equal. The wall is single-layered (autophragm), ~0.4 µm thick and light brown. The autophragm is smooth and sparsely ornamented with isolated sutural spinules usually forming interrupted low crests. Spinules are solid, generally ~2.0 µm long (few up to ~3.5 µm), and with broad bases and tapered to truncated tips. Linear crests with distinctively thickened bases incompletely reflect tabulation. Crests are well-developed on the apex, antapical horns, cingulum and sometimes along most of both lateral margins. The apex often bears ornamentation. The

apical horn is faintly developed by a thickening of the apex. Antapical horns are similar in length, slightly divergent and up to ~6.5 μm long. The antapical depression is shallow and wide. The cingulum is planar to slightly helicoidal, indicated by two folds and interrupted ventrally by an unornamented sulcal region. The cingular area, which is sometimes inflated, bears ornamentation from single spinules to continuous crests. The cingular ornamentation is evenly distributed along the anterior margin but unevenly distributed along the posterior margin, presumably reflecting tabulation. Cysts are weakly dorsoventrally compressed and 21 of the 57 specimens found are in polar orientation presumably due to post-depositional compression (Figure 6, 10–16). The archeopyle is hexagonal, formed by the release of the anterior intercalary plate 2a, and presumably isodeltalinteloid (Figure 6, 7–9). The operculum is free and sometimes adherent on adcingular margin.

Dimensions: Holotype: length, 52 μm; width, 56 μm. Range: length, 42–63 μm; width, 44–68 μm. Fifteen specimens measured.

Comparison: Cristadinium lucyae sp. nov. is distinguished from previously described *Cristadinium* species in having solid sutural spinules unevenly distributed over the entire cyst, which may be distally tapered to truncated, forming linear low crests with thickened bases and distally indented to serrated (Figure 4). *C. cristatoserratum* has a continuous sutural crests converging towards the apex and lacking scattered spines on the epicyst. *C. diminutivum* is smaller (~41 μm) and has angular outline. *C. headii* has distally acicular to bifid processes, and *C. striatiserratum* has nontabular striations. Single specimens reported as *C.* aff. *cristatoserratum* from the late Miocene of the Labrador Sea (Plate VII, 12, Head et al., 1989a), *Cristadinium* sp. 1 (Plate VII, 9, Head et

al., 1989a) and *Cristadinium* sp. 2 (Plate VII, 10, Head et al., 1989a) may belong to *C. lucyae* sp. nov.

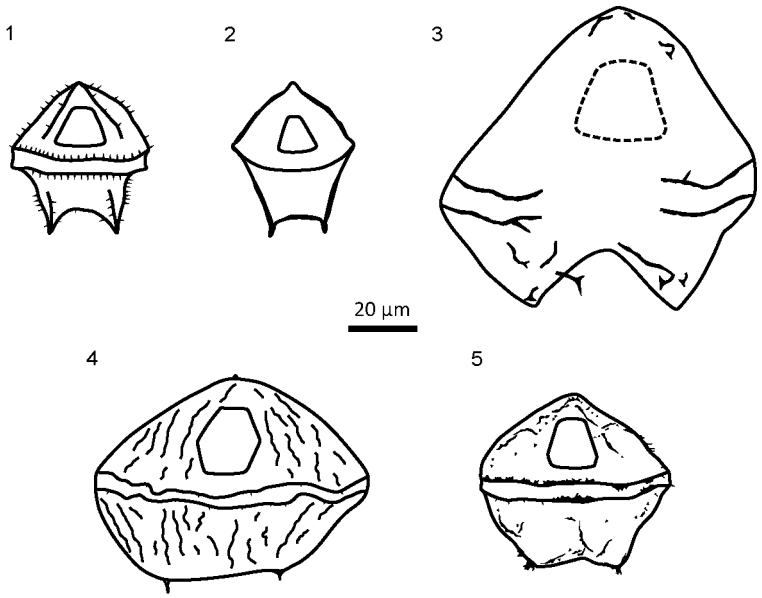

Figure 4. Schematic representation of *Cristadinium* taxa. 1. *C. cristatoserratum*. 2. *C. diminutivum*. 3. *C. headii*. 4. *C. lucyae* sp. nov.. 5. *C. striatiserratum*.

Mertens et al. (2017) interpreted as *Trinovantedinium pallidifulvum* the specimen depicted in de Verteuil and Norris (1992; Figure 7, 9–12) as an undefined protoperidiniacean. However, we consider that this specimen belongs to *Cristadinium lucyae* sp. nov.. While *T. pallidifulvum* is characterized by acuminate penitabular and intratabular ornamentation (Matsuoka, 1987; de Verteuil and Norris 1992; Mertens et al., 2017), de Verteuil and Norris (1992) reported sutural spinules, which are a key trait of *C. lucyae* sp. nov. Furthermore, the photomicrographs in de Verteuil and Norris (1992) and Edwards et al. (2018) show distally tapered and truncated (rarely branched) ornamentation, which are connected proximally, forming low crests especially along the

lateral margins and the cingulum (see de Verteuil and Norris 1992, p. 404–405; Edwards et al. 2018, p. 188–189).

Occurrence: Cristadinium lucyae sp. nov. was previously recorded in the Serravallian of the western North Atlantic as an undescribed protoperidiniacean species that may be attributable to *Cristadinium* (de Verteuil and Norris, 1992; Edwards et al., 2018). This species consistently occurs throughout the Aquitanian in the Cocinetas Basin, and an isolated occurrence was recorded in the Burdigalian (Figures 2–3).

Genus: *Trinovantedinium* Reid 1977 emended de Verteuil and Norris 1992

Type species: *Trinovantedinium applanatum* (Bradford 1977) Bujak and Davies 1983

Species: *Trinovantedinium uitpensis* sp. nov.

Figure 6, 17–20; Figure 7 1–11

Trinovantedinium sp., Cárdenas et al. 2020, Figures 9R, 9S

Etymology: In reference to the Uitpa Spring in La Guajira, Colombia, after which Renz (1960) named the Uitpa Formation in the Cocinetas Basin, where this species occurs and is first reported.

Locality: Cocinetas Basin, La Guajira, Colombia.

Holotype: Figure 7, 1–3, Slide STRI 42214, Sample Well A 2500'–2530', England Finder reference D38/1.

Repository: Instituto de Investigaciones en Estratigrafía, Universidad de Caldas, Colombia. Catalogue number UC-B214-IIES-D-044-060.

Stratigraphic horizon: Uitpa Formation.

Age: Aquitanian, early Miocene.

Diagnosis: Peridinioid cyst moderately dorsoventrally compressed, proximate, acavate. Pentagonal outline in dorsoventral view wider than long: straight to slightly convex epicyst with rounded apex; straight to slightly concave hypocyst with two antapical horns. Autophragm smooth with verrucate to slightly baculate penitabular ornamentation. Cingulum planar to slightly helicoidal with denticulated margins. Archeopyle intercalary hexa 2a, presumably isodeltalinteloid. Operculum free to adherent.

Description: Peridinioid cyst proximate, acavate and moderately dorsoventrally compressed with pentagonal outline in dorsoventral view: sides of the epicyst are straight to slightly convex, whereas sides of the hypocyst are straight to slightly concave. The cyst is wider than long, and therefore, five of the eight specimens found are in polar orientation presumably due to post-depositional compression (Figure 7, 4–11). Lengths of the epicyst and the hypocyst are approximately equal. The apex is rounded and the antapex has two slightly asymmetrical horns, up to ~12.5 µm long, distally tapering into rounded tips. The antapical depression is shallow and wide. The wall is single-layered (autophragm), ~0.4 µm thick and light brown in color. The autophragm is smooth with verrucate to slightly baculate penitabular ornamentation. Verrucae are solid, ~1.0 µm wide and ~1.0 µm long. Baculae are solid, ~1.0 µm wide and ~1.4 µm long. The cingulum is planar to slightly helicoidal, indicated by two denticulate folds and interrupted ventrally by an unornamented sulcal region. The cingular area may be slightly inflated. Cingular baculae are solid or hollow, usually connected proximally, ~1.0 µm wide and ~2.5 µm long. The archeopyle is formed by the release of the anterior

intercalary plate 2a and presumably hexagonal isodeltalinteloid (Figure 7, 8–9). The operculum is free and sometimes adherent on adcingular margin.

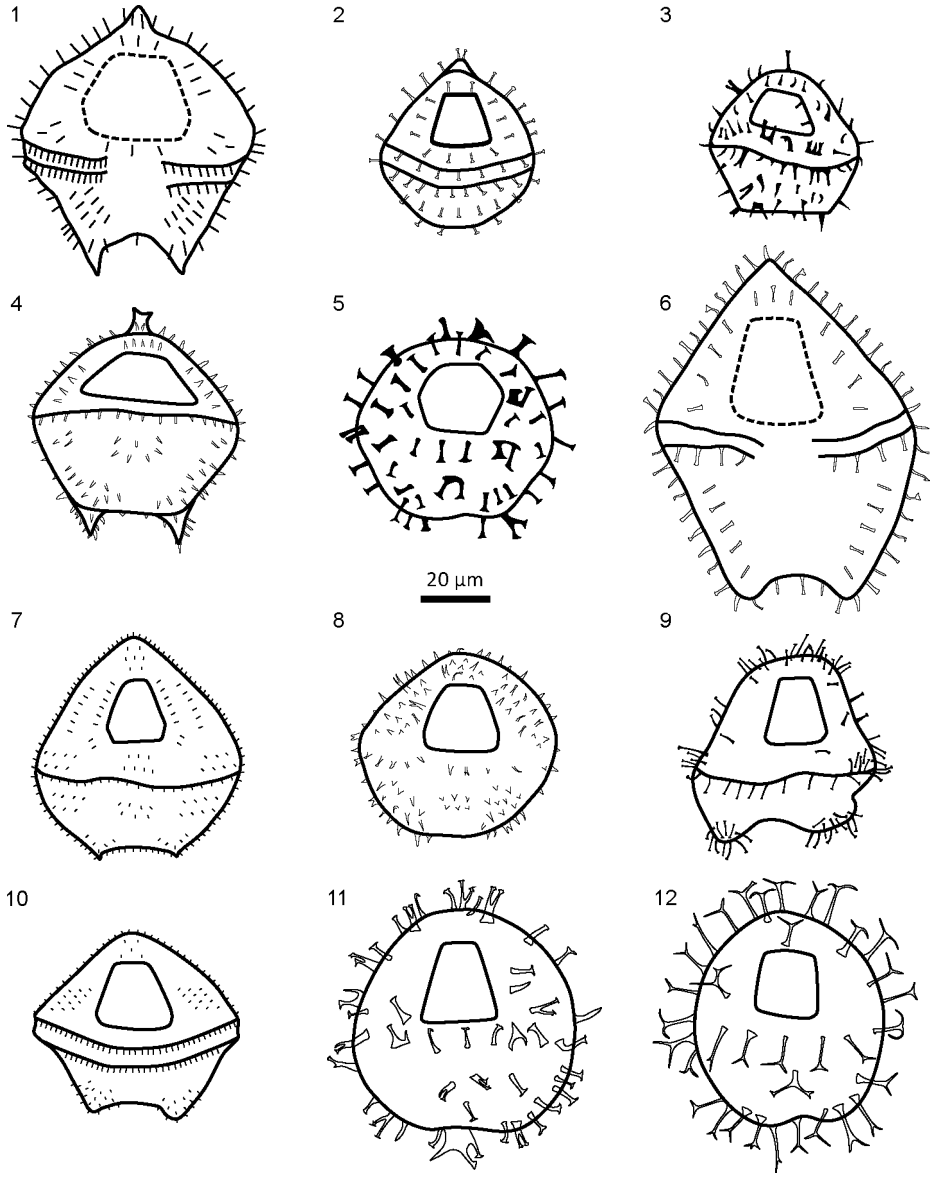

Figure 5. Schematic representation of *Trinovantedinium* taxa. 1. *T. applanatum*. 2. *T. boreale*. 3. *T. ferugnomatum*. 4. *T. glorianum*. 5. *T. harpagonium*. 6. *T. henrietii*. 7. *T. pallidifulvum*. 8. *T. papula*. 9. *T. sterthense*. 10. *T. uitpensis* sp. nov.. 11. *T. variabile*. 12. *T.? xylochoporum*.

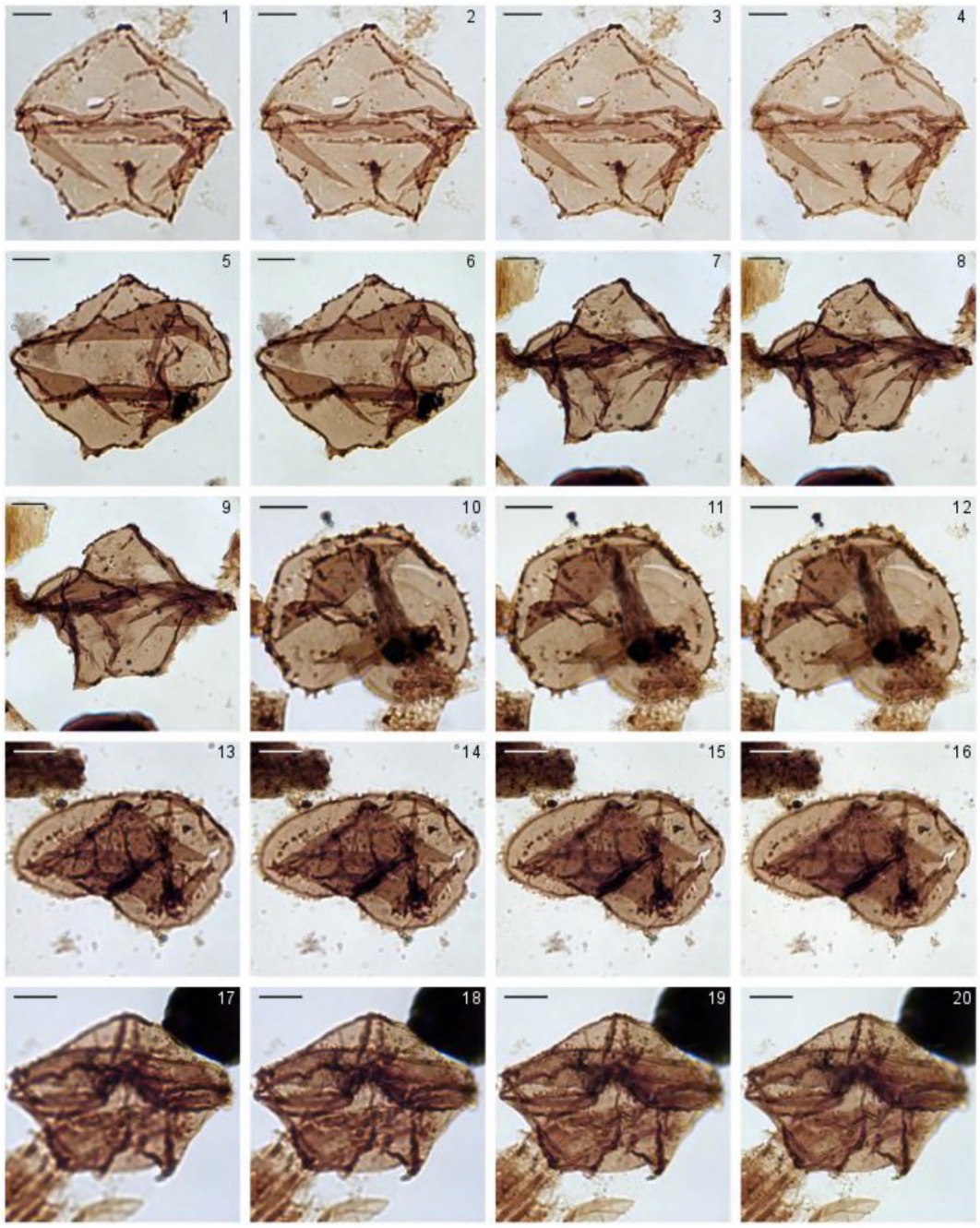

Figure 6. Photomicrographs of new marine palynomorph taxa from the Cocinetas Basin in northern Colombia, northwestern South America. Scale bar is 10 µm. 1–16. *Cristadinium lucyae* sp. nov.. 1–4. Holotype, STRI 42198, EF: K48/4, dorsal view at high, mid-high, mid-low and low foci. 5–6. Paratype, STRI 42191, EF: T33, dorsoventral view at high and low foci. 7–9. Paratype, STRI 42189, EF: V43/3 dorsal view at high, middle and low foci. 10–12. Paratype, STRI 42208, EF: O47/1, apical view at high, middle and low foci. 13–16. Paratype, STRI 42192, EF: N30/4, diagonal ventroapical view at high, mid-high, mid-low and low foci. 17–20. *Trinovantedinium uitpensis* sp.

nov., paratype, STRI 42200, EF: E42/3, ventral view at high, mid-high, mid-low and low foci.

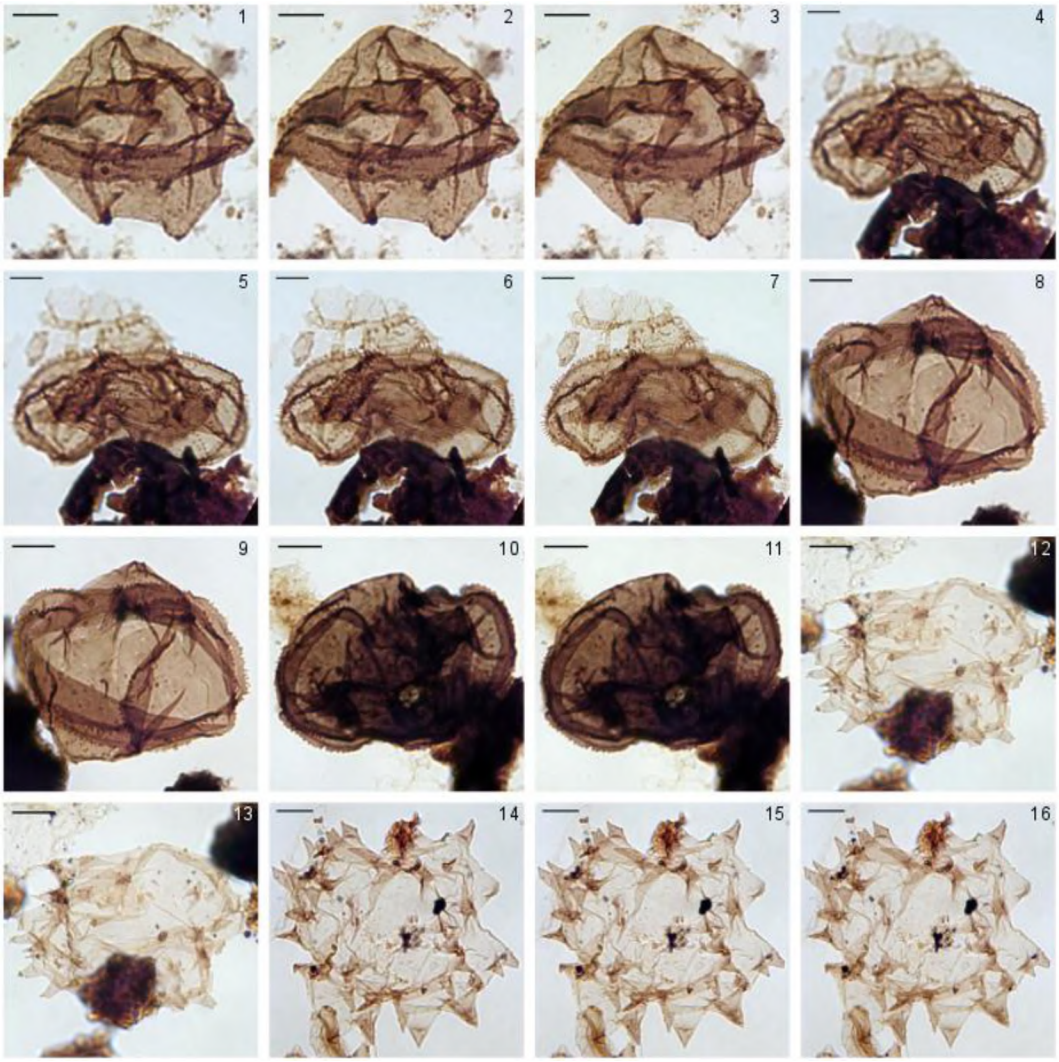

Figure 7. Photomicrographs of new marine palynomorph taxa from the Cocinetas Basin in northern Colombia, northwestern South America. Scale bar is 10 µm. 1–11. *Trinovantedinium uitpensis* sp. nov..1–3. Holotype, STRI 42214, EF: D38/1, dorsal view at high, middle and low foci. 4–7. Paratype, STRI 42198, EF: O41/2, antapical view at high, mid-high, mid-low and low foci. 8–9. Paratype, STRI 42212, EF: M40/1, diagonal dorsoapical view at high and low foci. 10–11. Paratype, STRI 42216, EF: L39, antapical? view at high and low foci. 12–16. *Quadrina*? *triangulata* sp. nov.. 12–13. Paratype, STRI 42157, EF: H31/2, uncertain view, at high and low foci. 14–16. Holotype, STRI 42142, EF: R37/2, uncertain view at high, middle and low foci.

Dimensions: Holotype: length, 48 µm; width, 53 µm. Range: length, 38–48 µm; width, 51–73 µm. Three specimens measured.

Comparison: Trinovantedinium uitpensis sp. nov. differs from other species in the genus by having denticulate cingulum and verrucate to slightly baculate ornamentation elsewhere (Figure 5). Ornamentation in species of *Trinovantedinium* vary as follows: *T. applanatum*: acuminate and slightly capitate; *T. boreale*: capitate; *T. ferugnomatum*: acuminate, capitate and bifid; *T. glorianum*: acuminate, truncated and occasionally bifid; *T. harpagonium*: taeniate and flared to infundibular; *T. henrietii*: flared; *T. pallidifulvum*: acuminate; *T. papula*: acuminate, capitate and rarely distally bifurcate; *T. sterthense*: capitate; *T. variabile*: considerable variation but mostly flared and aculeate, occasionally irregularly branched (see Bujak 1984, p. 194, Text-Figure 3); *T.*? *xylochoporum*: tubiform and tapering, distally ramified.

Occurrence: Trinovantedinium uitpensis sp. nov. sporadically occurs in the Aquitanian in the Cocinetas Basin (Figures 2–3).

Group ACRITARCHA Evitt 1963

Genus: *Quadrina* Bujak in Bujak et al. 1980

Type species: *Quadrina pallida* Bujak in Bujak et al. 1980

Species: *Quadrina*? *triangulata* sp. nov.

Figure 7, 12–16

Dinocyst XI, LeNoir and Hart 1986, Plate VII, 6

Quadrina "incerta", Jaramillo et al. 2017, Figure S5D; Jaramillo et al. 2020, Figure 5O; Cárdenas et al. 2020, Figure 7L

Etymology: From the Latin word *triangulatus*, in reference to the triangular profile of the processes.

Locality: Cocinetas Basin, La Guajira, Colombia.

Holotype: Figure 7, 14–16, Slide STRI 42142, Sample Well A 280'–310', England Finder reference R37/2.

Repository: Instituto de Investigaciones en Estratigrafía, Universidad de Caldas, Colombia. Catalogue number UC-B214-IIES-D-044-065.

Stratigraphic horizon: Jimol Formation.

Age: Burdigalian, early Miocene.

Diagnosis: Organic-walled microfossil with rectangular to cruciform outline. The wall is single-layered, smooth and light brown to pale. Conical to subconical processes predominantly distributed at the four corners. Polygonal pylome with free operculum.

Description: Single-layered acritarch with subrectangular to cruciform outline. The wall is smooth, ~0.4 µm thick and pale in the central body, ~0.5 µm and light brown in the processes. Processes are distinctively thickened, conical to subconical, hollow, distally closed, often with slightly ovoidal bases, ~4.0–8.5 µm long and ~3.5–8.5 µm wide at the base. Approximately 8–15 processes per corner. The pylome is polygonal, sometimes discernible and usually with a free operculum (Figure 7, 12–13; Figure S5D, Jaramillo et al., 2017). However, the position, extent and shape of the pylome are uncertain.

Dimensions: Holotype: length, 63 µm; width, 67 µm. Range: length, 56–68 µm; width, 59–73 µm. Three specimens measured.

Comparison: Quadrina? *triangulata* sp. nov. differs from previously described *Quadrina* taxa in process shape: acuminate or capitate in *Q*.? *condita* and acuminate in *Q. pallida*.

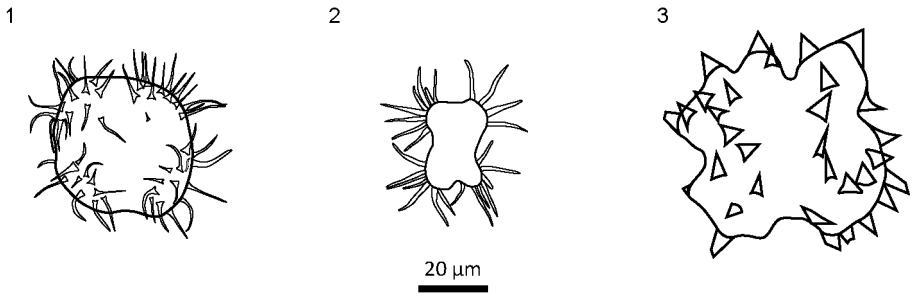

Figure 8. Schematic representation of *Quadrina* taxa. 1. *Q*.? *condita*. 2. *Q. pallida*. 3. *Q*.? *triangulata* sp. nov..

The fossil genus *Quadrina* was erected by Bujak (in Bujak et al. 1980) to accommodate compressed acritarchs with subrectangular outline bearing groups of tapered processes at the four corners of the cyst. Bujak described a single species, *Quadrina pallida*, from Eocene deposits in England. Subsequently, de Verteuil and Norris (1992) described *Quadrina*? *condita* from the Miocene of the United States east coast. De Verteuil and Norris noted that *Q*.? *condita* was probably a dinoflagellate cyst and thus provisionally assigned this species to the acritarch genus *Quadrina*. Although *Q*.? *condita* lacks discernible tabulation, its morphological features suggest that this species is likely a protoperidiniacean dinoflagellate cyst (de Verteuil and Norris, 1992; Soliman et al., 2012).

We assign *Q*.? *triangulata* sp. nov. to the genus *Quadrina* due to its overall morphological resemblance to previously described taxa in this fossil acritarch genus. However, our assignment is provisional because this new species may represent a

protoperidiniacean dinoflagellate cyst mostly due to its thin brown-colored walled, size and morphology. The absence of discernible tabulation under light microscopy requires further examination of morphological characters using scanning electron microscopy, specifically the excystment structure. Consequently, while beyond the scope of this work, detailed morphological analysis of *Quadrina*? *condita* and *Quadrina*? *triangulata* sp. nov. is necessary to better understand its taxonomy.

Occurrence: Quadrina? *triangulata* sp. nov. was previously recorded as Dinocyst XI from the late Burdigalian of the Gulf of Mexico (LeNoir and Hart, 1986), and the mid-Burdigalian of northwestern South America as *Quadrina* "incerta" (Jaramillo et al., 2017). This species occurs sporadically throughout the middle and late Burdigalian in the Cocinetas Basin (Figures 2–3).

5. CONCLUSIONS

Three new marine palynomorph taxa, namely two peridinioid dinoflagellate cysts, *Cristadinium lucyae* sp. nov. and *Trinovantedinium uitpensis* sp. nov., and the acritarch *Quadrina*? *triangulata* sp. nov. are formally described.

Cristadinium lucyae sp. nov. and *Trinovantedinium uitpensis* sp. nov. occur during the Aquitanian in northwesternmost South America. *C. lucyae* sp. nov.is more abundant and has also been recorded in the Serravallian of the western North Atlantic. These two new dinoflagellate cyst taxa improve our understanding of protoperidiniacean taxonomic diversity.

The acritarch *Quadrina*? *triangulata* sp. nov. occurs sporadically during the middle and late Burdigalian in northwestern South America, and represents a potential key biostratigraphic marker for the Burdigalian in the tropical Americas.

Future studies are needed not only to further constrain the distribution of these three new taxa through space and time but also to decipher their paleoenvironmental significance.

ACKNOWLEDGMENTS

We especially thank Claudia Correa (INVEMAR, Colombia) for enhancing the geologic map, Lucy Edwards (USGS, Reston) for taxonomic discussions, and Andrés Pardo (IIES, Colombia) for housing the type species. We also acknowledge the Colombian National Hydrocarbons Agency for providing access to the Well A samples. Sincere thanks to Martin Head and one anonymous reviewer for providing insightful comments that improved the quality of the manuscript. We are grateful to journal editor Michael Stephenson for handling the manuscript. Partial funding was provided by the Geological Society of America (GSA Graduate Student Research Grant) and the Paleontological Society (Yochelson Student Research Award).

APPENDIX

Supplementary material related to this article can be found online at https://doi.org/10.1016/j.palaeo.2020.109955

REFERENCES

Bujak, J.P., 1984. Cenozoic Dinoflagellate Cysts and Acritarchs from the Bering Sea and Northern North Pacific, DSDP Leg 19. Micropaleontology 30, 180–212. https://doi.org/10.2307/1485717

Bujak, J.P., Downie, C., Eaton, G.L., Williams, G.L., 1980. Dinoflagellate Cysts and Acritarchs from the Eocene of Southern England. Special Papers in Palaeontology 24.

Cárdenas, D., Jaramillo, C., Oboh-Ikuenobe, F., 2020. Early Miocene marine palynology of the Colombian Caribbean Margin: biostratigraphic and paleoceanographic implications. Palaeogeogr. Palaeoclimatol. Palaeoecol. 558, 109955. https://doi.org/https://doi.org/10.1016/j.palaeo.2020.109955

Carrillo-Briceño, J.D., Argyriou, T., Zapata, V., Kindlimann, R., Jaramillo, C., 2016. A New Early Miocene (Aquitanian) Elasmobranchii Assemblage from the la Guajira Peninsula, Colombia. Ameghiniana 53, 77–99.

de Verteuil, L., Norris, G., 1992. Miocene protoperidiniacean dinoflagellate cysts from the Maryland and Virginia coastal plain, in: Head, M.J., Wrenn, J.H. (Eds.), Neogene and Quaternary Dinoflagellate Cysts and Acritarchs. American Asociation of Stratigraphic Palynologists Foundation, pp. 391–430.

Edwards, L.E., Weems, R.E., Carter, M.W., Spears, D.B., Powars, D.S., 2018. The significance of dinoflagellates in the Miocene Choptank Formation beneath the Midlothian gravels in the southeastern Virginia Piedmont. Stratigraphy 15, 179–195. https://doi.org/10.29041/strat.15.179-195

Fensome, R.A., Taylor, F.J.R., Norris, G., Sarjeant, W.A.S., Wharton, D.I., Williams, G.L., 1993. A classification of fossil and living dinoflagellates. Micropaleontology Press Special Paper No. 7.

Fensome, R.A., Williams, G.L., MacRae, R.A., 2019. The Lentin and Williams Index of fossil dinoflagellates. American Association of Stratigraphic Palynologysts Foundation, Contribution Series No. 50.

Head, M.J., Norris, G., Mudie, P.J., 1989. Palynology and dinocyst stratigraphy of the Miocene in ODP LEG 105, HOLE 645E, Baffin Bay, in: Srivastava, S.P., Arthur, M.A., Clement, B., Aksu, A., Baldauf, J., Bohrmann, G., Busch, W., Cederberg, T., Cremer, M., Dadey, K., Vernal, A. De, Firth, J., Hall, F., Head, M., Hiscott, R., Jarrard, R., Kaminski, M., Lazarus, D., Monjanel, A.-L., Nielsen, O.B., Stein, R., Thiebault, F., Zachos, J., Zimmerman, H. (Eds.), Proceedings of the Ocean Drilling Program, Scientific Results Volume 105. pp. 467–514.

Hendy, A.J.W., Jones, D.S., Moreno, F., Zapata, V., Jaramillo, C., 2015. Neogene molluscs, shallow marine paleoenvironments, and chronostratigraphy of the Guajira Peninsula, Colombia. Swiss J. Palaeontol. 134, 45–75. https://doi.org/10.1007/s13358-015-0074-1

Jaramillo, C., Moreno, F., Hendy, A.J.W., Sánchez-Villagra, M.R., Marty, D., 2015. Preface: La Guajira, Colombia: a new window into the Cenozoic neotropical biodiversity and the Great American Biotic Interchange. Swiss J. Palaeontol. 134, 1–4. https://doi.org/10.1007/s13358-015-0075-0

Jaramillo, C., Romero, I., D'Apolito, C., Bayona, G., Duarte, E., Louwye, S., Escobar, J., Luque, J., Carrillo-Briceño, J.D., Zapata, V., Mora, A., Schouten, S., Zavada, M., Harrington, G., Ortiz, J., Wesselingh, F.P., 2017. Miocene flooding events of western Amazonia. Sci. Adv. 3, e1601693. https://doi.org/10.1126/sciadv.1601693

Jaramillo, C., Sepulchre, P., Cárdenas, D., Correa-Metrio, A., Moreno, J.E., Trejos, R., Vallejos, D., Hoyos, N., Martínez, C., Carvalho, D., Escobar, J., Oboh-Ikuenobe, F., Prámparo, M.B., Pinzón, D., 2020. Drastic Vegetation Change in La Guajira Peninsula (Colombia) during the Neogene. Paleoceanogr. Paleoclimatology. 35, e2020PA003933. https://doi.org/10.1029/2020PA003933

LeNoir, E.A., Hart, G.F., 1986. Burdigalian (Early Miocene) dinocysts from offshore Louisiana, in: Wrenn, J.H., Duffield, S.L., Stein, J.A. (Eds.), Papers from the First Symposium on Neogene Dinoflagellate Cyst Biostratigraphy. American Asociation of Stratigraphic Palynologists Contribution Series No. 17, pp. 59–81.

Macellari, C.E., 1995. Cenozoic Sedimentation and Tectonics of the Southwestern Caribbean Pull-Apart Basin, Venezuela and Colombia, in: Tankard, A.J., Soruco, R.S., Welsink, H.J. (Eds.), Petroleum Basins of South America. American Association of Petroleum Geologists, pp. 757–780. https://doi.org/10.1306/M62593C41

Matsuoka, K., 1987. Organic-walled dinoflagellate cysts from surface sediments of Akkeshi Bay and Lake Saroma, north Japan. Bull. Fac. Lib. Arts, Nagasaki Univ. Nat. Sci. 28, 35–123.

Mertens, K.N., Gu, H., Takano, Y., Price, A.M., Pospelova, V., Bogus, K., Versteegh, G.J.M., Marret, F., Turner, R.E., Rabalais, N.N., Matsuoka, K., 2017. The cyst-theca relationship of the dinoflagellate cyst Trinovantedinium pallidifulvum, with erection of Protoperidinium lousianensis sp. nov. and their phylogenetic position within the Conica group. Palynology 41, 183–202. https://doi.org/10.1080/01916122.2016.1147219

Moreno, F., Hendy, A.J.W., Quiroz, L., Hoyos, N., Jones, D.S., Zapata, V., Zapata, S., Ballen, G.A., Cadena, E., Cárdenas, A.L., Carrillo-Briceño, J.D., Carrillo, J.D., Delgado-Sierra, D., Escobar, J., Martínez, J.I., Martínez, C., Montes, C., Moreno, J., Pérez, N., Sánchez, R., Suárez, C., Vallejo-Pareja, M.C., Jaramillo, C., 2015. Revised stratigraphy of Neogene strata in the Cocinetas Basin, La Guajira, Colombia. Swiss J. Palaeontol. 134, 5–43. https://doi.org/10.1007/s13358-015-0071-4

Renz, O., 1960. Geología de la parte sureste de la peninsula de La Guajira. III Congr. Geológico Venez. Boletín Geol. Publicación Espec. Minist. Minas e Hidrocarburos 3, 317–347.

Soliman, A., Ćorić, S., Head, M.J., Piller, W.E., Beialy, S.Y. El, 2012. Lower and Middle Miocene biostratigraphy, Gulf of Suez, Egypt based on dinoflagellate cysts and calcareous nannofossils. Palynology 36, 38–79. https://doi.org/10.1080/01916122.2011.633632

Stover, L.E., Evitt, W.R., 1978. Analyses of pre-Pleistocene organic-walled dinoflagellates. Stanford University Publication in Geological Sciences No. 15.

Turland, N.J., Wiersema, J.H., Barrie, F.R., Greuter, W., Hawksworth, D.L., Herendeen, P.S., Knapp, S., Kusber, W.-H., Li, D.-Z., Marhold, K., May, T.W., McNeill, J., Monro, A.M., Prado, J., Price, M.J., Smith, G.F., 2018. International Code of Nomenclature for algae, fungi, and plants (Shenzhen Code) adopted by the Nineteenth International Botanical Congress Shenzhen, China, July 2017.

Williams, G.L., Fensome, R.A., Miller, M.A., Sarjeant, W.A.S., 2000. A glossary of the terminology applied to dinoflagellates, acritarchs and prasinophytes, with emphasis on fossils. American Asociation of Stratigraphic Palynologists Contribution Series No. 37.

Wood, G.D., Gabriel, A.M., Lawson, J.C., 1996. Palynological techniques – processing and microscopy, in: Jansonius, J., McGregor, D.C. (Eds.), Palynology: Principles and Applications, Volume 1. AASP – The Palynological Society, Dallas, Texas, pp. 29–50.

SECTION

2. CONCLUSIONS

A biostratigraphic scheme is proposed for the early Miocene in the Colombian Caribbean Margin, comprising an upper Chattian–lower Aquitanian *Minisphaeridium latirictum* Interval Zone (~23.9–22.0 Ma), an upper Aquitanian *Achomosphaera alcicornu* Interval Zone (~22.0–20.3 Ma), and a Burdigalian *Cribroperidinium tenuitabulatum* Interval Zone (~20.3–17.5 Ma).

A sudden shift from peridinioid-dominated to gonyaulacoid-dominated dinoflagellate cyst assemblages near the Aquitanian–Burdigalian boundary (~20.7 Ma), which indicates a rapid and permanent drop in marine primary productivity in the Colombian Caribbean Margin, was likely related to the initial constriction of the Central American Seaway during the early Miocene.

Two peridinioid dinoflagellate cysts, *Cristadinium lucyae* sp. nov. and *Trinovantedinium uitpensis* sp. nov., and the acritarch *Quadrina*? *triangulata* sp. nov. are formally described.

Quadrina? *triangulata* sp. nov. representens a potential key biostratigraphic marker for the Burdigalian in the tropical Americas.

VITA

Damián Cárdenas Loboguerrero was born in Bogotá, Colombia. He received his Bachelor of Science degree in Geology in 2012 from the Geosciences Department at the National University of Colombia. Damián received his PhD degree in Geology and Geophysics in the Department of Geosciences and Geological and Petroleum Engineering at the Missouri University of Science and Technology (Missouri S&T) in May 2021. He worked as a junior palynologist at the Colombian Petroleum Institute from 2013 to 2015. Damián was also an intern (2015–2017) and a predoctoral fellow (2020–2021) at the Smithsonian Tropical Research Institute in Panama. During his PhD at Missouri S&T, he worked as a graduate assistant from 2017 to 2021. In 2020, Damián was elected to serve a two-year office position as student Director-at-Large by AASP – The Palynological Society.